Table I. *LMIR3 WT or different mutants*[a]

Abbreviation	Residues at 241, 276, 289, 303, 325
WT	Y241, Y276, Y289, Y303, Y325
Y1F	F241, Y276, Y289, Y303, Y325
Y2F	Y241, F276, Y289, Y303, Y325
Y3F	Y241, Y276, F289, Y303, Y325
Y4F	Y241, Y276, Y289, F303, Y325
Y5F	Y241, Y276, Y289, Y303, F325
Y1/3F	F241, Y276, F289, Y303, Y325
Y1/5F	F241, Y276, Y289, Y303, F325
Y3/5F	Y241, Y276, F289, Y303, F325
Y1/3/5F	F241, Y276, F289, Y303, F325
Y2/4/5F or 1/3Y	Y241, F276, Y289, F303, F325
Y2/3/4F or 1/5Y	Y241, F276, F289, F303, Y325
Y1/2/4F or 3/5Y	F241, F276, Y289, F303, Y325
Y2/4F or 1/3/5Y	Y241, F276, Y289, F303, Y325
Y2/3/4/5F or 1Y	Y241, F276, F289, F303, F325
Y1/3/4/5F or 2Y	F241, Y276, F289, F303, F325
Y1/2/4/5F or 3Y	F241, F276, Y289, F303, F325
Y1/2/3/5F or 4Y	F241, F276, F289, Y303, F325
Y1/2/3/4F or 5Y	F241, F276, F289, F303, Y325
Y1/2/3/4/5F or YallF	F241, F276, F289, F303, F325

[a] LMIR3 cytoplasmic tyrosine residues, Y241, Y276, Y289, Y303, and Y325 are abbreviated as Y1, Y2, Y3, Y4, and Y5, respectively. In LMIR3 mutants, single or several tyrosine residues (Y) were replaced with phenylalanine (F).

Y4 are not important for the inhibitory function of LMIR3. On the other hand, LMIR3(Y1F), (Y3F), or (Y5F) mutant-mediated inhibition was only 45–60% when compared with LMIR3(WT)-mediated inhibition. In the LMIR3(Y1/3F) mutant where both Y1 and Y3 located in ITIM were replaced with phenylalanine, the inhibition was 30%. Coligation of FcεRI and LMIR3(Y1/3/5F) mutant, where Y5 located in ITSM in addition to Y1/3 was replaced with phenylalanine, did not result in the inhibition of IL-6 production at all. Collectively, these results indicated that the inhibitory effect of LMIR3 on FcεRI-mediated cytokine production was dependent on both ITIM and ITSM in the cytoplasmic region.

LMIR3 associated with SHP-1 and SHP-2 via phosphorylated Y241, Y289, and Y325, while associating with the p85 subunit of PI3K via phosphorylated Y276

We next explored which molecules LMIR3 associated with through the phosphorylation of its cytoplasmic tyrosine residues. When FLAG-tagged LMIR3(WT)-transduced Ba/F3 cells were stimulated by sodium pervanadate, Western blot analysis displayed a mobility shift of tyrosine-phosphorylated LMIR3 (Fig. 3*A*, *left panel*). Generally, ITIM can associate with phosphatases such as SHP-1, SHP-2, or SHIP, while ITSM can bind not only to phosphatases but also to the p85 regulatory subunit of PI3K or to other adaptor molecules, depending on receptor type and cellular context (22, 23). Moreover, Y276 or Y303 fits the putative binding motif for p85 or Grb2, respectively. Therefore, we performed coimmunoprecipitation experiments using LMIR3(WT)-transduced Ba/F3 cells stimulated by sodium pervanadate. Immunoprecipitates of lysates with anti-FLAG Ab were subjected to probing with anti-SHP-1, SHP-2, SHIP, p85, or Grb2 Ab, demonstrating that tyrosine-phosphorylated LMIR3 associated with SHP-1 or SHP-2, but not with SHIP, among phosphatases, and with p85 or Grb2 (Fig. 3*A*, *middle panel*). Because Grb2 was not easy to discern from the nonspecific Ig L chain due to the similar mobilities in the Western blot, immunoprecipitates of lysates with anti-Grb2 Ab were also probed with anti-LMIR3 Ab, confirming that Grb2 associated with phosphorylated LMIR3 (Fig. 3*A*, *right panel*). Moreover, similar results that tyrosine-phosphorylated LMIR3 associated with SHP-1, SHP-2, or p85 were also obtained by coimmunoprecipitation experiments using LMIR3(WT)-transduced BMMCs (supplemental Fig. S3). To further explore the contribution of each tyrosine residue to the association of LMIR3 with SHP-1, SHP-2, or p85, different LMIR3 mutant-transduced Ba/F3 cells were generated. Equivalent expression levels of surface LMIR3 were confirmed among different transfectants by using anti-FLAG Ab (supplemental Fig. 4). We also performed coimmunoprecipitation experiments on Ba/F3 transfectants expressing the mutants. The association of LMIR3 with SHP-1, SHP-2, or p85 as well as tyrosine phosphorylation and concomitant mobility shift of LMIR3 upon sodium pervanadate stimulation was abolished by the replacement of all five tyrosine residues with phenylalanine in the cytoplasmic LMIR3 (Fig. 3*B*, *left panel*). This confirmed that tyrosine phosphorylation of LMIR3 was necessary for the association of LMIR3 with SHP-1, SHP-2, or p85. As shown in Fig. 3*B*, only LMIR3(Y2F) mutant did not coimmunoprecipitate p85 among LMIR3 mutants where a single tyrosine residue was replaced with phenylalanine (*left panel*). In parallel, only LMIR3(2Y) mutant coimmunoprecipitated p85 among LMIR3 mutants where four of five tyrosine residues were replaced with phenylalanine, at levels comparable to LMIR3(WT) (Fig. 3*B*, *right panel*). Thus, Y276 was indispensable for the association of LMIR3 with p85. On the other hand, the association of LMIR3 with SHP-1 or SHP-2 was slightly reduced in LMIR3(Y1F), (Y3F), or (Y5F) mutants (Fig. 3*B*, *right panel*), while LMIR3(1Y), (3Y), or (5Y) mutant did not coimmunoprecipitate SHP-1 or SHP-2 at all (Fig. 3*B*, *right panel*). These results suggested that the combination of Y1, Y3, or Y5 is required for the association. Analysis of LMIR3(Y1/3F), (Y1/5F), (Y3/5F), (Y1/3/5F), (1/3Y), (1/5Y), (3/5Y), or (1/3/5Y) mutant demonstrated that Y1/3/5(> Y1/5 > Y3/5 > Y1/3 in order) played a critical role in the association of LMIR3 with SHP-1 or SHP-2 (Fig. 3*C*), which was in accordance with the finding that Y1, Y3, and Y5 are required for the maximum inhibitory effect of LMIR3 on FcεRI-mediated cytokine production (Fig. 2*E*).

Crosslinking of LMIR3(Y241/276/289/303/325/F) mutant as well as LMIR3(Y241/289/325/F) mutant resulted in IL-6 production in the transduced BMMCs

The potential of LMIR3 to associate with p85 or Grb2 via its tyrosine phosphorylation prompted us to postulate that LMIR3 could transmit an activating signal, at least in LMIR3 mutants that lost the inhibitory function. In fact, cytokine production of the transduced BMMCs was strongly induced by crosslinking of LMIR3(Y1/3/5F) mutant that had lost the inhibitory function (Fig. 4*A*). Consistently, engagement of LMIR3(Y1/3F) mutant that partially lost the inhibitory function resulted in lower but significant levels of IL-6 production compared with that of LMIR3(Y1/3/5F) mutant (Fig. 4*A*). Moreover, Western blot analysis demonstrated that crosslinking of LMIR3(Y1/3/5F) in the transduced BMMCs induced the tyrosine phosphorylation of LMIR3 and the association of LMIR3 with p85, suggesting the importance of Y2 and Y4 in the activating role of LMIR3 (Fig. 4*C*). In contrast, cytokine production was not significantly induced by crosslinkng of LMIR3(WT) or LMIR3(Y1F), (Y2F), (Y3F), (Y4F), (Y5F), (Y2/4F), or (Y2/4/5F) mutants (Fig. 4*A*). Collectively, these results are consistent with the finding recently reported by Alvarez-Errico et al. on IREM-1/human LMIR3 that both Y236 and Y263 in IREM-1 played an important part in IREM-1-mediated activating signal (25). Furthermore, similar experiments were conducted on LMIR1, another ITIM-containing receptor among the LMIR family. In BMMCs transduced with LMIR1(WT) or LMIR1(Y258/270F) mutant in which the inhibitory function was disrupted by the replacement

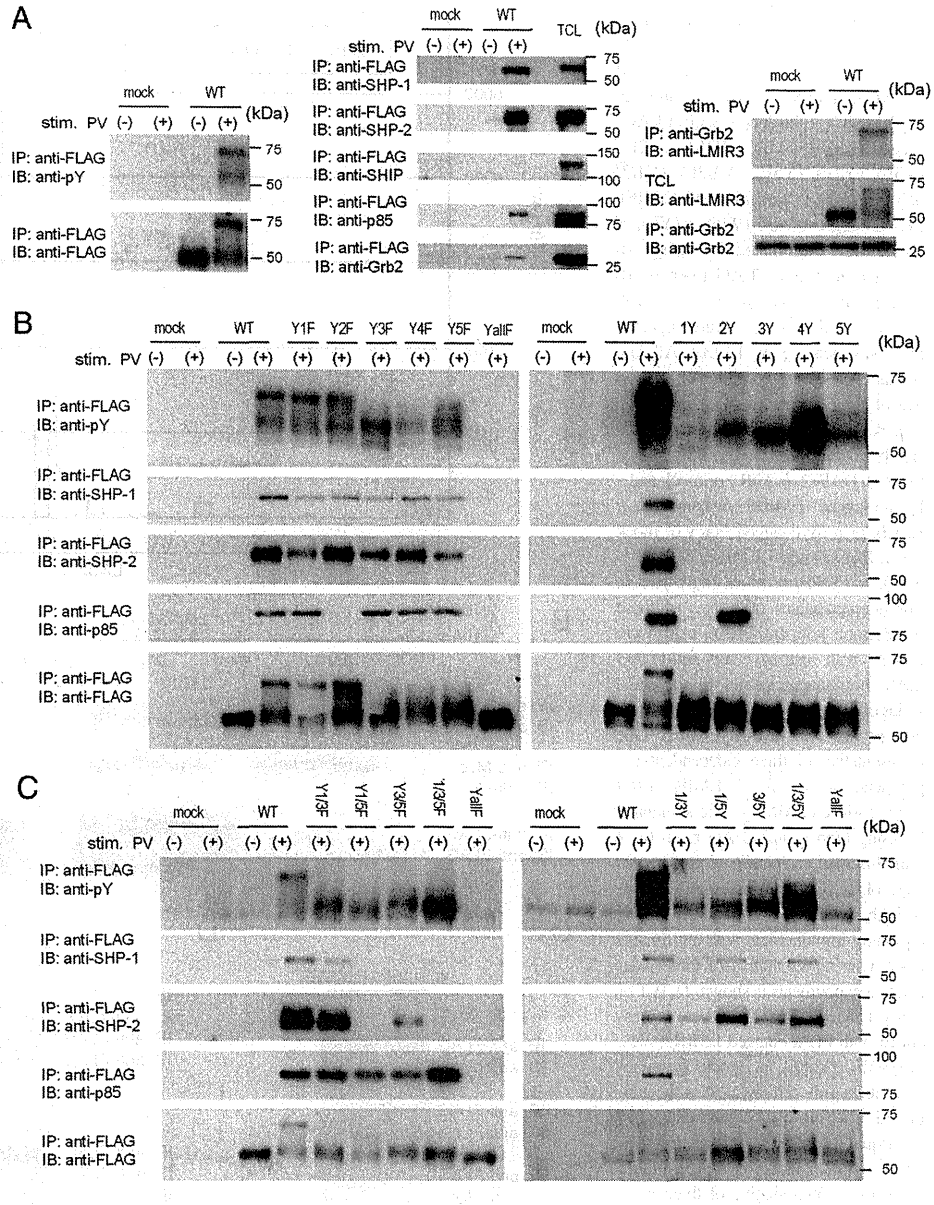

FIGURE 3. LMIR3 associates with SHP-1 or SHP-2 via Y241/289/325, while it does so with p85α via Y276. *A*, Ba/F3 cells transduced with FLAG-tagged LMIR3(WT) or mock were stimulated or not with 100 μM sodium pervanadate. Immunoprecipitates of cell lysates with rabbit anti-FLAG Ab or total cell lysates were blotted with anti-phosphotyrosine (pY) mAb or anti-FLAG mAb (*left panel*), anti-SHP-1 Ab, anti-SHP-2 Ab, anti-SHIP Ab, anti-p85 Ab, or anti-Grb2 Ab (*middle panel*). Alternatively, immunoprecipitates of cell lysates with anti-Grb2 Ab were blotted with anti-LMIR3 Ab or anti-Grb2 Ab, and total cell lysates were blotted with anti-LMIR3 Ab (*right panel*). *B* and *C*, Ba/F3 cells transduced with FLAG-tagged LMIR3 WT, different mutants, or mock were stimulated or not with 100 μM sodium pervanadate. Immunoprecipitates of cell lysates with rabbit anti-FLAG Ab were blotted with anti-pY mAb, anti-SHP-1 Ab, anti-SHP-2 Ab, anti-p85 Ab, or anti-FLAG mAb. *B*, Ba/F3 cells transduced with FLAG-tagged LMIR3(WT), (Y1F), (Y2F), (Y3F), (Y4F), (Y5F), or mock (*left panel*) or with FLAG-tagged LMIR3(WT), (1Y), (2Y), (3Y), (4Y), (5Y), or mock (*right panel*) were used. *C*, Ba/F3 cells transduced with LMIR3(WT), (Y1/3F), (Y1/5F), (Y3/5F), (Y1/3/5F), (YallF), or mock (*left panel*) or with LMIR3(WT), (1/3Y), (1/5Y), (3/5Y), (1/3/5Y), (YallF), or mock (*right panel*) were used. Data are representative of three independent experiments. TCL and VO_4 indicate total cell lysates and sodium pervanadate, respectively.

of both Y258 and Y270 situated in ITIM with phenylalanine (21), comparable surface expression levels of LMIR1 as well as mast cell maturity were confirmed as well (supplemental Fig. 2). When either transfectant was stimulated by LMIR1 crosslinking, we found no detectable levels of cytokine production (Fig. 4*A*), indicating the specificity of LMIR3-mediated activation events. However, unlike the results for IREM-1, crosslinking of LMIR3(YallF) mutant that did not contain phosphorylatable tyrosine residues led to the production of a significant level of IL-6 in the transduced BMMCs. These results let us postulate the potential of LMIR3 to transmit an activating signal independent of its cytoplsmic tyrosine residues.

LMIR3 associated with FcRγ, but not DAP10 or DAP12, in BMMCs

To clarify the mechanism of LMIR3-mediated activating signal independent of LMIR3 tyrosine phosphorylation (Fig. 4*A*), we attempted to test the possibility that LMIR3 associated with FcRγ, DAP10, or DAP12, although it was unlikely that ITIM-containing inhibitory receptors associated with ITAM- or the related activating motif-bearing adaptor molecules. Surprisingly, coimmunoprecipitation experiments using COS-7 cells cotransduced with LMIR3(WT) and either Myc-tagged FcRγ, DAP10, DAP12, or mock clearly demonstrated that LMIR3 associated with FcRγ, but not DAP10 or DAP12 (Fig. 4*B*, *left panel*). Similar coimmunoprecipitation experiments also revealed that not only LMIR3(WT) but also LMIR3(Y1/3/5F) or LMIR3(YallF) mutant associated with FcRγ (Fig. 4*B*, *right panel*), suggesting that the association of LMIR3 with FcRγ was independent of tyrosine residues of LMIR3. Additionally, in either WT or FcRγ-deficient BMMCs transduced with LMIR3(WT), (Y1/3/5F) mutant, or (YallF) mutant, we confirmed the association of LMIR3, irrespective of WT or mutants, with endogenous FcRγ in mast cells (Fig. 4*D*). Collectively, an inhibitory receptor LMIR3 associated with FcRγ in mast cells.

FcRγ played a critical role in LMIR3-mediated cytokine production in LMIR3(Y241/289/325F) or (Y241/276/289/303/325F) mutant-transduced BMMCs

As shown in Fig. 5*A*, equivalent surface expression levels of c-kit with no detectable FcεRI were observed in FcRγ-deficient

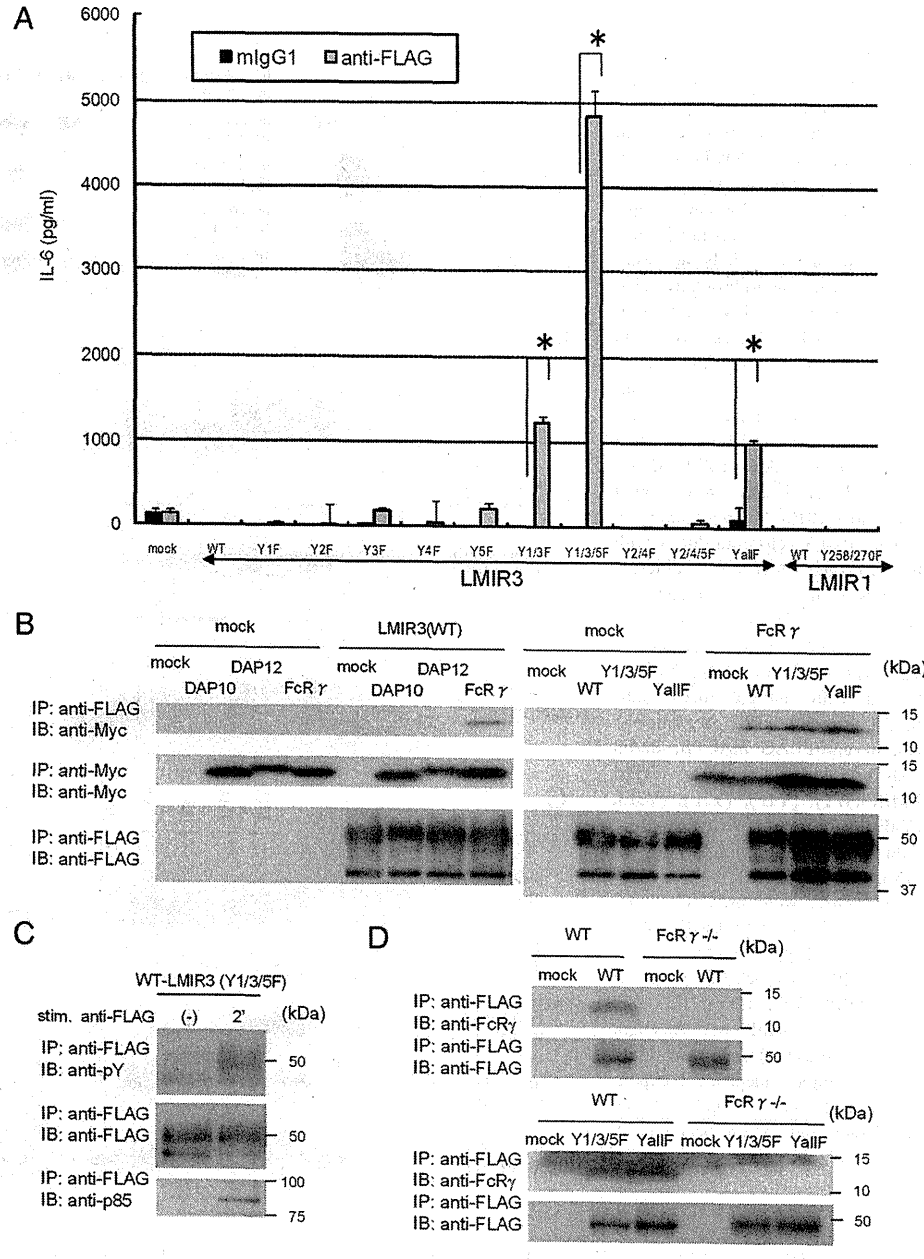

FIGURE 4. Crosslinking of LMIR3-(Y241/289/325F) or LMIR3(Y241/276/289/303/325F) in the transduced BMMCs induced cytokine production. *A*, BMMCs transduced with FLAG-tagged LMIR3(WT), (Y1F), (Y2F), (Y3F), (Y4F), (Y5F), (Y1/3F), (Y1/3/5F), (Y2/4F), (Y2/4/5F), or (YallF), FLAG-tagged LMIR1(WT) or (YF), or mock were stimulated by using 10 μg/ml $F(ab')_2$ anti-FLAG mAb or 10 μg/ml mouse IgG1 mAb as control. IL-6 released into the culture supernatants was measured by ELISA. All data points correspond to the mean and the SD of three independent experiments. *, $p < 0.05$. *B*, COS-7 cells were transiently cotransduced with a Myc-tagged DAP10, DAP12, or FcRγ or mock and a FLAG-tagged LMIR3 or mock (*left panel*), or a Myc-tagged FcRγ or mock and a FLAG-tagged LMIR3(WT), (Y1/3/5F), or (YallF) or mock (*right panel*). Immunoprecipitates of lysates of these transfectants with anti-FLAG mAb were probed with anti-Myc or anti-FLAG mAb. Immunoprecipitates of the same series of lysates with anti-Myc mAb were also probed with anti-Myc mAb. One representative of three independent experiments is shown. *C*, LMIR3(Y1/3/5F)-transduced BMMCs were stimulated by using $F(ab')_2$ anti-FLAG mAb for 2 min. Immunoprecipitates of cell lysates were blotted with anti-pY mAb or anti-p85 Ab. Equal loading was evaluated by reprobing immunoblots with anti-FLAG mAb. One representative of three independent experiments is shown. *D*, WT or FcRγ-deficient BMMCs were transduced with FLAG-tagged LMIR3(WT), (Y1/3/5F), (YallF), or mock. Immunoprecipitates of cell lysates with anti-FLAG Ab were blotted with anti-FcRγ Ab. Equal loading was evaluated by reprobing immunoblots with anti-FLAG mAb. One representative of three independent experiments is shown.

BMMCs transduced with LMIR3(WT), (Y1/3/5F) mutant, (YallF) mutant, or mock (26). When surface expression levels of LMIR3(WT) or mutants were compared between WT and FcRγ-deficient BMMCs, no significant difference was observed, suggesting that FcRγ was dispensable for efficient surface expression of LMIR3 in BMMCs despite its association with LMIR3 (Fig. 5*A*). To clarify the role of FcRγ in the activating function of LMIR3, we measured the amounts of IL-6 released from LMIR3(Y1/3/5F)-transduced WT or FcRγ-deficient BMMCs stimulated by LMIR3 crosslinking. Notably, the deficiency of FcRγ severely, but not completely, impaired IL-6 production of the transduced BMMCs stimulated by LMIR3 crosslinking. As expected, the deficiency of FcRγ completely abolished IgE-dependent IL-6 production, although PMA stimulation led to comparable amounts of IL-6 production in both transfectants (Fig. 5*B*). In accordance with this, FcRγ deficiency caused severe impairment of both ERK and Akt activation in the transduced BMMCs stimulated by crosslinking of LMIR3(Y1/3/5F) (Fig. 5*C*). Next, similar experiments were performed in WT and FcRγ-deficient BMMCs transduced with LMIR3(YallF) mutant. Strikingly, the absence of FcRγ completely dampened IL-6 production of the transduced BMMCs stimulated by crosslinking of LMIR3(YallF) mutant as well as by IgE, although PMA as a control produced comparable levels of IL-6 irrespective of the presence or absence of FcRγ (Fig. 5*D*). Collectively, these results suggested that FcRγ played a predominant role in cytokine production of BMMCs stimulated by crosslinking of LMIR3(Y1/3/5F) or (YallF) mutant.

Crosslinking of LMIR3 enhanced cytokine production of BMMCs triggered by TLR4 agonist, while it suppressed that stimulated by other TLR agonists or SCF

Since the potential of LMIR3 to transmit an activating signal in mast cells had been demonstrated, we next attempted to find the physiological situation where LMIR3 functions as an activating receptor. Intriguingly, crosslinking of LMIR3 dramatically enhanced cytokine production of LMIR3(WT)-transduced BMMCs

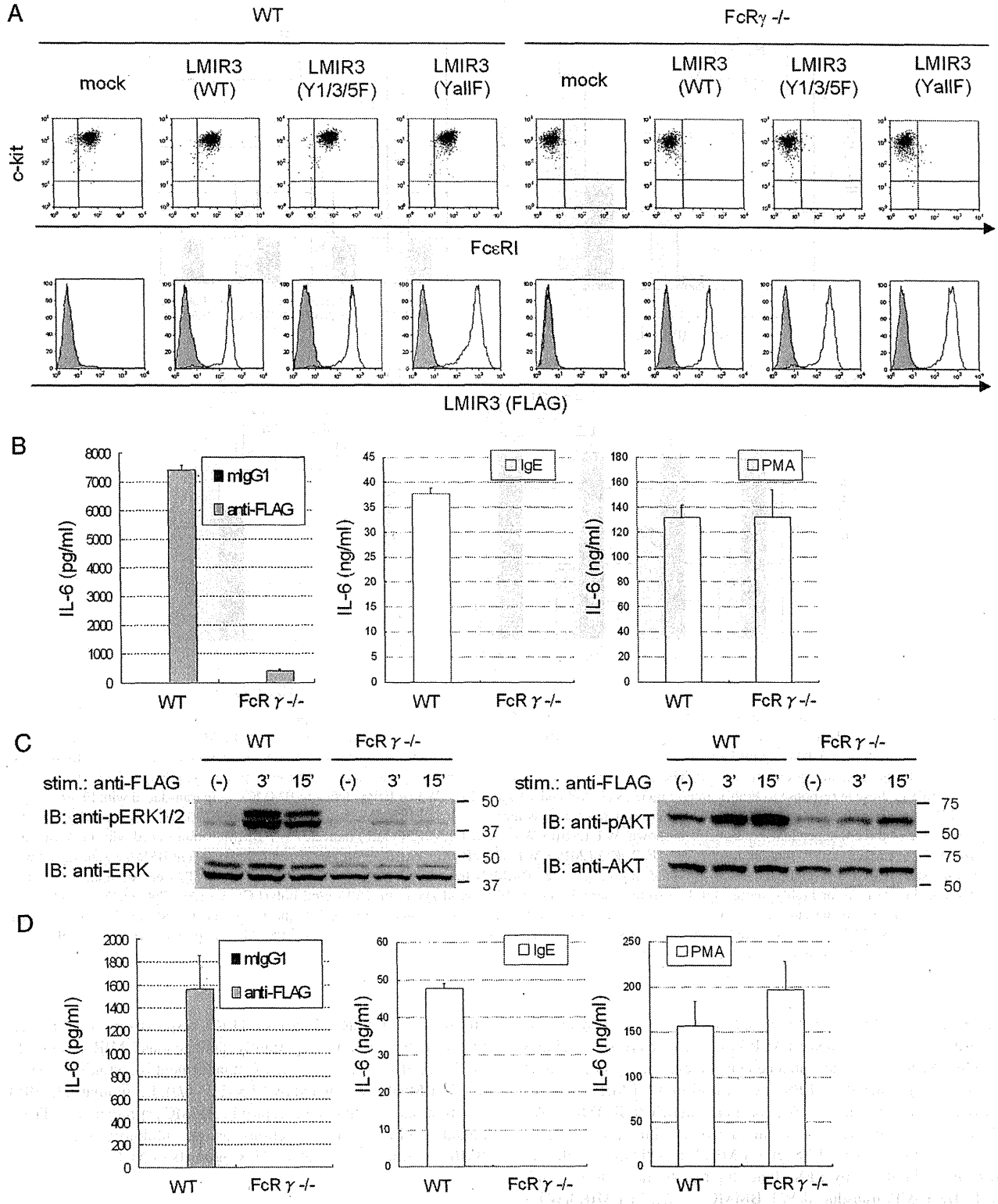

FIGURE 5. Cytokine production of the transduced BMMCs induced by engagement of LMIR3(Y241/289/325F) or LMIR3(Y241/276/289/303/325F) is severely or completely, respectively, impaired by FcRγ deficiency. *A*, WT or FcRγ-deficient BMMCs were transduced with FLAG-tagged LMIR3(WT), (Y1/3/5F) mutant, (YallF) mutant, or mock. Surface expression levels of c-kit and IgE-bound FcεRI as well as those of FLAG-tagged LMIR3 were analyzed by flow cytometry. *B* and *D*, WT or FcRγ-deficient BMMCs transduced with LMIR3(Y1/3/5F) (*B*) or LMIR3(YallF) (*D*) were stimulated by $F(ab')_2$ anti-FLAG mAb or $F(ab')_2$ mouse IgG1 as control (*left panel*), SPE-7 IgE (*middle panel*), or PMA (*right panel*). IL-6 released into the culture supernatants was measured by ELISA. All data points correspond to the mean and the SD of four independent experiments. *C*, WT or FcRγ-deficient BMMCs transduced with LMIR3(Y1/3/5F) were stimulated by $F(ab')_2$ anti-FLAG mAb for the indicated times. Cell lysates were subject to immunoblotting with anti-phospho-p44/42 MAPK (pERK1/2) Ab (*left panel*) or anti-phospho-Akt Ab (*right panel*). Equal loading was evaluated by reprobing the immunoblots with anti-ERK1/2 Ab (*left panel*) or anti-Akt Ab (*right panel*). One representative of three independent experiments is shown.

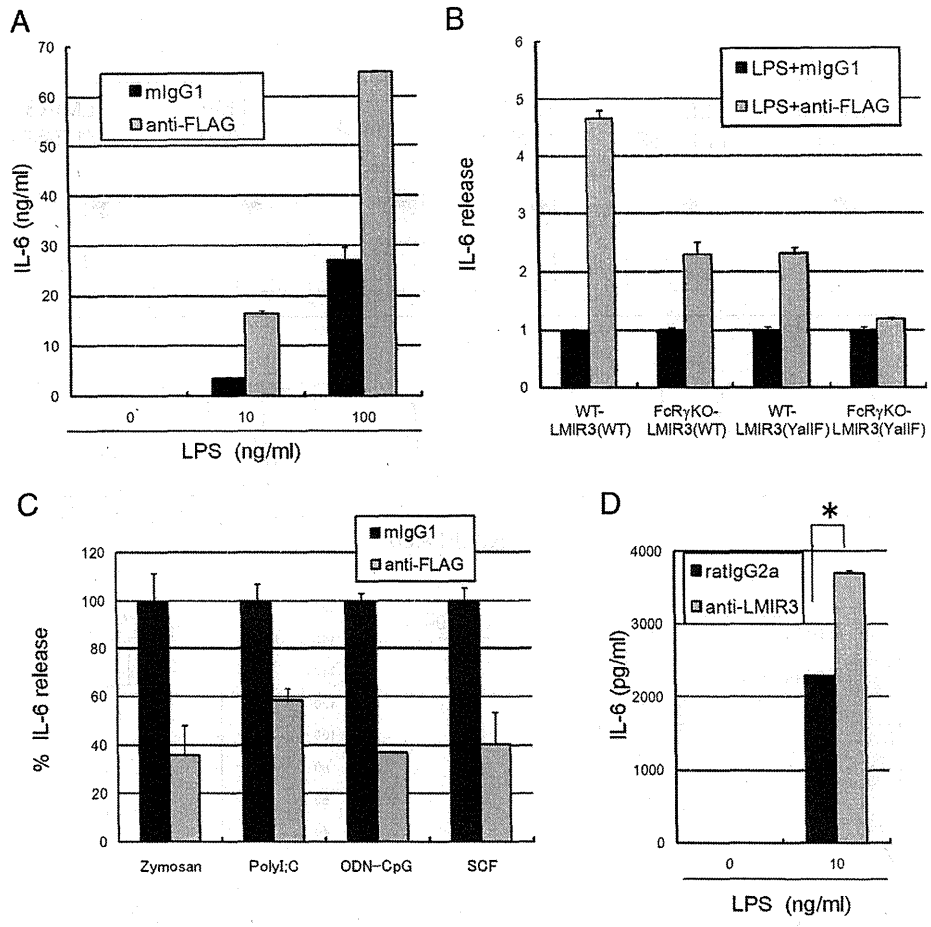

FIGURE 6. LMIR3 crosslinking enhances cytokine production of BMMCs stimulated by LPS, while suppressing that stimulated by zymosan, poly(I:C), CpG0ODN, or SCF. *A*, BMMCs transduced with FLAG-tagged LMIR3(WT) were stimulated by either $F(ab')_2$ anti-FLAG mAb or $F(ab')_2$ mouse IgG1 mAb together with 0, 10, or 1000 ng/ml LPS. IL-6 released into the culture supernatants was measured by ELISA. All data points correspond to the mean and the SD of four independent experiments. *B*, The ratio of the amounts of IL-6 released by each transfectant in response to $F(ab')_2$ anti-FLAG mAb and 10 ng/ml LPS to those in response to $F(ab')_2$ mouse IgG1 as control and 10 ng/ml LPS. WT or FcRγ-deficient BMMCs were transduced with FLAG-tagged LMIR3(WT) or (YallF). IL-6 released into the culture supernatants was measured by ELISA. All data points correspond to the mean and the SD. One representative of three independent experiments is shown. WT-LMIR3(WT) or WT-LMIR3(YallF) indicates WT BMMCs transduced with FLAG-tagged LMIR3(WT) or LMIR3(YallF) mutant, respectively. FcRγKO-LMIR3(WT) or FcRγKO-LMIR3(YalF) indicates FcRγ-deficient BMMCs transduced with FLAG-tagged LMIR3(WT) or LMIR3(YallF) mutant, respectively. *C*, BMMCs transduced with FLAG-tagged LMIR3(WT) were stimulated by either $F(ab')_2$ anti-FLAG mAb or $F(ab')_2$ mouse IgG1 mAb together with either 100 μg/ml zymosan, 250 μg/ml poly(I:C), 5 μg/ml CpG-ODN, or 100 ng/ml SCF. IL-6 released into the culture supernatants was measured by ELISA. All data points correspond to the mean and the SD of three independent experiments. *D*, BMMCs were stimulated either anti-LMIR3 Ab or rat IgG2a together or not with 10 ng/ml LPS. All data points correspond to the mean and the SD of four independent experiments. *, $p < 0.05$.

stimulated by LPS, a TLR4 ligand (Fig. 6*A*). To delineate the contribution of FcRγ and/or LMIR3 cytoplasmic tyrosine residues to the LMIR3-mediated enhancement of cytokine production of mast cells stimulated by LPS, we utilized either LMIR3(WT) or LMIR3(YallF)-transduced WT or FcRγ-deficient BMMCs. We then measured the ratio of the amount of cytokine production in BMMCs stimulated by LPS plus LMIR3 crosslinking to that in BMMCs stimulated by LPS alone, finding the ratios to be ~4.7 in LMIR3(WT)-transduced WT BMMCs, ~2.2 in LMIR3(WT)-transduced FcRγ-deficient BMMCs, ~2.2 in LMIR3(YallF)-transduced WT BMMCs, or ~1.1 in LMIR3(YallF)-transduced FcRγ-deficient BMMCs. Taken together, these results indicated that both FcRγ and LMIR3 cytoplasmic tyrosine residues played an important role in LMIR3-mediated enhancement of cytokine production of BMMCs stimulated by LPS (Fig. 6*B*). In contrast, LMIR3 crosslinking impaired cytokine production of LMIR3-transduced BMMC stimulated by zymosan, poly(I:C), or CpG-ODN, which are ligands for TLR2, TLR3, or TLR9, respectively, or SCF (Fig. 6*C*). Finally, and most importantly, endogenous LMIR3 crosslinking induced significant levels of enhancement of cytokine production in BMMCs stimulated by LPS (Fig. 6*D*). In summary, LMIR3 functions as an activating receptor in BMMCs stimulated by TLR4 ligand, while LMIR3 functions as an inhibitory receptor in BMMCs stimulated by other TLR agonists or SCF.

Discussion

The biological role of paired immune receptors remains incompletely understood, but recent advances postulate their main functions in innate immunity. Paired activating receptors respond rapidly and effectively to foreign pathogens such as bacteria or viruses, while paired inhibitory receptors suppress the steady-state response to self proteins or excessive inflammation under pathological conditions. Generally, the former associate with ITAM or

ITAM-related activating motif-bearing adaptor molecules to transmit an activating signal, while the latter contain ITIM in the cytoplasmic region to transmit an inhibitory signal (1, 2, 27, 28). On the other hand, growing evidence has recently established the concept of dual functionality of an immune receptor that is related to the concept of inhibitory ITAM or activating ITIM (29–34). In fact, some ITAM-containing receptors can deliver an inhibitory signal in a cell type and stimulation-dependent manner, as exemplified by the inhibitory effect of triggering receptor expressed on myeloid cells 2 (TREM-2) on LPS response (35, 36) or FcαRI on monomeric IgA response (37). Conversely, ITIM-containing receptors transmitting an activating signal are rare, but, for example, platelet-endothelial cell adhesion molecule-1 (PECAM-1) can promote endothelial cell migration (38). Additionally, ITSM-containing receptors, such as SLAM family immunoreceptors, also exhibit dual functionality (23). For instance, 2B4 (CD244)-mediated NK cell activity was promoted or suppressed by the association of its ITSM with SH2D1A or EAT-2, respectively (39).

In the present study, we delineated the dual function of LMIR3 in mast cells. As expected from the structural characteristic that LMIR3 contains two ITIMs in the cytoplasmic region, LMIR3 exerted an inhibitory effect on FcεRI-mediated cytokine production in mast cells. However, analysis of different LMIR3 mutants demonstrated that the maximum inhibitory function as well as the maximum association of LMIR3 with SHP-1 or SHP-2 required an ITSM (including Y5) in addition to two ITIMs (including Y1 and Y3) (Fig. 2*E*). Remarkably, both Y1 and Y5 (Y1/5) played a predominant role (Y1/5 > Y3/5 > Y1/3) in the association of LMIR3 with SHP-1 or SHP-2, while a single tyrosine residue (Y1, Y3, or Y5) had a minimum role. These results strongly suggested an indispensable role of ITSM and the differential roles of two ITIMs in the inhibitory function of LMIR3. However, adaptor molecules with positive functions to associate with LMIR3 via its ITSM might be able to interfere with the inhibitory function of LMIR3. Additionally, how SHP-1 and SHP-2 differentially contribute to LMIR3-mediated inhibition in mast cells remains to be resolved.

On the other hand, the potential of ITIM-containing LMIR3 to function as an activating receptor was illustrated by experimental results that in mast cells, crosslinking of LMIR3(Y1/3/5F) mutant lacking the inhibitory function induced high amounts of cytokine production (Fig. 4*A*) as well as the activation of ERK and Akt (Fig. 5*C*) and the association of p85 with phosphorylated LMIR3(Y1/3/5F) (Fig. 4*D*). In support of this, LMIR3 associated with p85 exclusively via phosphorylated Y2 (Fig. 3*B*). Therefore, it is anticipated that PI3K will be important to the LMIR3-mediated activating pathway. Additionally, the association of LMIR3 with Grb2 was also recognized (Fig. 3*A*), but LMIR3 tyrosine residues responsible for the binding could not be identified (data not shown) notwithstanding the fact that Y4 is located in the binding motif for Grb2. This might be either because Grb2 is not easy to discriminate from Ig L chain in coimmunoprecipitation experiments or because LMIR3 associates with Grb2 but not necessarily via Y4. Further examination is necessary, but the association of LMIR3 with Grb2 should lead to the activation of Ras/ERK in the LMIR3-mediated activating pathway. Indeed, these results do not always conflict with recent reports on IREM-1/human LMIR3, but there exists the striking difference between mouse and human LMIR3. Unlike IREM-1, crosslinking of LMIR3(YallF), in which all cytoplasmic tyrosine residues were replaced with phenylalanine, still induced significant levels of cytokine production in mast cells. We then asked if there exists an LMIR3-mediated activating signaling pathway independent of LMIR3 cytoplasmic tyrosine residues, and concluded that LMIR3 associates with ITAM-bearing FcRγ, thereby transmitting an activating signal in mast cells independently of tyrosines. Since LMIR3 contains no charged residues in the transmembrane domain, the association of LMIR3 with FcRγ appears not to be through pairwise interaction of basic and acidic residues. Related to this, surface expression levels of LMIR3, unlike typical activating receptors associating with FcRγ, were not affected by FcRγ deficiency. Simultaneously, we also found that cytokine production induced by triggering LMIR3(Y1/3/5F) or LMIR3(YallF) mutant, with the former being at much higher levels than the latter, was severely or completely, respectively, suppressed by FcRγ deficiency. This suggested that FcRγ played a predominant role as compared with Y2/4 of LMIR3 in LMIR3-mediated cytokine production. With the exception that killer cell Ig-like receptor (KIR)2DL4 contains ITIM in the cytoplasmic domain and a basic transmembrane residue through which it associates with FcRγ, LMIR3 is unusual in that an ITIM-containing receptor associates with an ITAM-bearing adaptor. Intriguingly, KIR2DL4 functions only as an activating receptor despite its bearing ITIM, whereas LMIR3 can function as either an inhibitory receptor via ITIM and ITSM or an activating receptor via Y276/303 and association with FcRγ. Additionally, several differences exist between mouse and human LMIR3. 1) IREM-1 associated with p85 via Y236 and Y263, both of which fit the binding motif for p85, while mouse LMIR3 did so only via Y2 (Fig. 3*B*). 2) Membrane-proximal ITIM played a predominant role in the inhibitory function of IREM-1, whereas ITSM did so in the case of LMIR3 (Figs. 2*E* and 3). 3) IREM-1 associated with SHP-1, but not SHP-2, while LMIR3 associated with both SHP-1 and SHP-2 (Fig. 3). 4) Coligation of IREM-1 and FcεRI in RBL cells induced an inhibition of the release of β-hexosaminidase, a marker of degranulation, while coligation of mouse LMIR3 and FcεRI in BMMCs led to the impairment of cytokine production, but not significant degranulation (Fig. 1 and data not shown). The difference might be explained by the different experimental systems including the quality of Ab used. On the other hand, because degranulation requires stronger FcεRI aggregation than cytokine production in BMMCs, a stronger inhibitory signal may be necessary for the inhibition of degranulation as compared with cytokine production (13, 41, 42). Accordingly, it is possible that mouse LMIR3 has relatively weaker inhibitory activities in comparison to human LMIR3, while having stronger activating activities via FcRγ in mast cells. From this point of view, the potential of mouse, but not human, LMIR3 to associate with SHP-2 might influence the magnitude of the inhibitory signal.

Most importantly, we found physiological conditions under which LMIR3 functions as an activating receptor in mast cells. As clearly demonstrated in Fig. 6, cytokine production of mast cells stimulated by LPS was profoundly enhanced by LMIR3 engagement, where the activating effect of LMIR3 on TLR4 signaling was dependent on FcRγ and LMIR3 cytoplasmic tyrosine residues. Considering that TLR4 expressed in mast cells plays a critical protective role in a model of acute septic peritonitis (43–45), LMIR3 signaling may either protect against enterobacterial infection or, conversely, cause prolonged excessive inflammation by enhancing the TLR4 signal. On the other hand, cytokine production of mast cells stimulated by SCF or other TLR agonists such as zymosan, poly(I:C), or CpG-ODN was impaired by LMIR3 crosslinking, although these stimuli did not affect surface expression levels of LMIR3 in mast cells (Fig. 6 and data not shown). Interestingly, these inhibitory events did not require coengagement of LMIR3 and TLRs or c-kit, whereas the inhibition of FcεRI signaling required coengagement of LMIR3 and FcεRI. In fact, the inhibition was not significantly observed when FcεRI and LMIR3 were engaged by anti-TNP IgE plus TNP-BSA and anti-LMIR3

Ab, respectively; that is, FcεRI and LMIR3 were separately engaged (data not shown). Collectively, the quality and quantity of stimuli may determine the function of LMIR3 as well as the phosphorylation levels of each LMIR3 tyrosine residue. The generation of Ab specific for each phosphorylated tyrosine of LMIR3 will give a clue to the stimulation-dependent LMIR3 function. To clarify the precise mechanism under which LMIR3 functions as an activating or inhibitory receptor is an important issue. Whether LMIR3 associates with TLR, where LMIR3- and TLR-mediated signaling pathways are combined, and how the quality and quantity of stimuli modulate the function of LMIR3 are all questions that remain to be resolved. In any case, LMIR3 can positively or negatively regulate TLR responses in mast cells, strongly suggesting the involvement of LMIR3 in the modulation of innate immunity. In view of the regulation of an activating and inhibitory signal in the immune system, the dual functionality of LMIR3 and its relevant mechanism presented here is unique and intriguing. Based on the counterbalance theory for evolution and function of paired receptors (46), we could hypothesize an in vivo function of LMIR3 as follows: if any pathogen utilized an inhibitory receptor LMIR3 to down-regulate responses against itself, another activating LMIR might have evolved to interact with it and thereby act as a counterbalance. Simultaneously, LMIR3 also might have evolutionally acquired the activating function to enhance TLR4 signal. Under normal conditions, LMIR3 constitutively inhibits weak signals in the steady-state from cytokine/chemokine or self-Ag through binding to an unknown endogenous ligand. Consequently, appropriate myeloid cell differentiation, distribution, and activation will be maintained, and the occurrence of autoimmune diseases will be avoided. Although both identification of a ligand for LMIR3 and analysis of LMIR3-deficient mice are indispensable to fully understand the function of LMIR3, this study will lead to the delineation of a novel aspect of immune regulation.

In conclusion, this study provides the first demonstration that an inhibitory receptor LMIR3 associates with FcRγ and thereby enhances LPS response in mast cells. Dual functions of LMIR3 are expected to play an important part in maintaining homeostasis and in responding to emergencies in immunity.

Acknowledgments

We thank Dr. Hisashi Arase for providing pME18S expression vector containing a mouse CD150 leader segment (43). We are grateful to Dr. Dovie Wylie for her excellent language assistance.

Disclosures

Toshio Kitamura serves as a consultant for R&D Systems.

References

1. Ravetch, J. V., and L. L. Lanier. 2000. Immune inhibitory receptors. *Science* 290: 84–89.
2. Takai, T., and M. Ono. 2001. Activating and inhibitory nature of the murine paired immunoglobulin-like receptor family. *Immunol. Rev.* 181: 215–222.
3. Kumagai, H., T. Oki, K. Tamitsu, S. Z. Feng, M. Ono, H. Nakajima, Y. C. Bao, Y. Kawakami, K. Nagayoshi, N. G. Copeland, et al. 2003. Identification and characterization of a new pair of immunoglobulin-like receptors LMIR1 and 2 derived from murine bone marrow-derived mast cells. *Biochem. Biophys. Res. Commun.* 307: 719–729.
4. Izawa, K., J. Kitaura, Y. Yamanishi, T. Matsuoka, T. Oki, F. Shibata, H. Kumagai, H. Nakajima, M. Maeda-Yamamoto, J. P. Hauchins, et al. 2007. Functional analysis of an activating receptor LMIR4 as a counterpart of an inhibitory receptor LMIR3. *J. Biol. Chem.* 282: 17997–18008.
5. Yamanishi, Y., J. Kitaura, K. Izawa, T. Matsuoka, T. Oki, Y. Lu, F. Shibata, S. Yamazaki, H. Kumagai, H. Nakajima, et al. 2008. Analysis of mouse LMIR5/CLM-7 as an activating recptor: differential regulation of LMIR5/CLM-7 in mouse versus human cells. *Blood* 111: 688–698.
6. Chung, D. H., M. B. Humphrey, M. C. Nakamura, D. G. Ginzinger, W. E. Seaman, and M. R. Daws. 2003. CMRF-35-like molecule-1, a novel mouse myeloid receptor, can inhibit osteoclast formation. *J. Immunol.* 171: 6541–6548.
7. Yotsumoto, K., Y. Okoshi, K. Shibuya, S. Yamazaki, S. Tahara-Hanaoka, S. Honda, M. Osawa, A. Kuroiwa, Y. Matsuda, D. G. Tenen, et al. 2003. Paired activating and inhibitory immunoglobulin-like receptors, MAIR-I and MAIR-II, regulate mast cell and macrophage activation. *J. Exp. Med.* 198: 223–233.
8. Luo, K., W. Zhang, L. Sui, N. Li, M. Zhang, X. Ma, L. Zhang, and X. Cao. 2001. DIgR1, a novel membrane receptor of the immunoglobulin gene superfamily, is preferentially expressed by antigen-presenting cells. *Biochem. Biophys. Res. Commun.* 287: 35–41.
9. Daish, A., G. C. Starling, J. L. McKenzie, J. C. Nimmo, D. G. Jackson, and D. N. Hart. 1993. Expression of the CMRF-35 antigen, a new member of the immunoglobulin gene superfamily, is differentially regulated on leukocytes. *Immunology* 79: 55–63.
10. Can, I., S. Tahara-Hanaoka, K. Hitomi, T. Nakano, C. Nakahashi-Oda, N. Kurita, S. Honda, K. Shibuya, and A. Shibuya. 2008. Caspase-independent cell death by CD300LF (MAIR-V), an inhibitory immunoglobulin-like receptor on myeloid cells. *J. Immunol.* 180: 207–213.
11. Shi, L., K. Luo, D. Xia, T. Chen, G. Chen, Y. Jiang, N. Li, and X. Cao. 2006. DIgR2, dendritic cell-derived immunoglobulin receptor 2, is one representative of a family of IgSF inhibitory receptors and mediates negative regulation of dendritic cell-initiated antigen-specific T-cell responses. *Blood* 108: 2678–2686.
12. Fujimoto, M., H. Takatsu, and H. Ohno. 2006. CMRF-35-like molecule-5 constitutes novel paired receptors, with CMRF-35-like molecule-1, to transduce activation signal upon association with FcRγ. *Int. Immunol.* 18: 1499–1508.
13. Kawakami, T., and S. J. Galli. 2002. Regulation of mast cell and basophil function and survival. *Nat. Rev. Immunol.* 2: 773–786.
14. Galli, S. J., S. Nakae, and M. Tsai. 2005. Mast cells in the development of adaptive immune responses. *Nat. Immunol.* 6: 135–142.
15. Kraft, S., and J. P. Kinet. 2007. New developments in FcεRI regulation, function and inhibition. *Nat. Rev. Immunol.* 7: 365–378.
16. Daëron, M., S. Latour, O. Malbec, E. Espinosa, P Pina, S. Pasmans, and W. H. Fridman. 1995. The same tyrosine-based inhibition motif, in the intracytoplasmic domain of FcγRIIB, regulates negatively BCR-, TCR-, and FcR-dependent cell activation. *Immunity* 3: 635–646.
17. Katz, H. R., E. Vivier, M. C. Castells, M. J. McCormick, J. M. Chambers, and K. F. Austen. 1996. Mouse mast cell gp49B1 contains two immunoreceptor tyrosine-based inhibition motifs and suppresses mast cell activation when coligated with the high-affinity Fc receptor for IgE. *Proc. Natl. Acad. Sci. USA* 93: 10809–10814.
18. Uehara, T., M. Bléry, D. W. Kang, C. C. Chen, L. H. Ho, G. L. Gartland, F. T. Liu, E. Vivier, M. D. Cooper, and H. Kubagawa. 2001. Inhibition of IgE-mediated mast cell activation by the paired Ig-like receptor PIR-B. *J. Clin. Invest.* 108: 1041–1050.
19. Yamashita, Y., M. Ono, and T. Takai. 1998. Inhibitory and stimulatory functions of paired Ig-like receptor (PIR) family in RBL-2H3 cells. *J. Immunol.* 161: 4042–4047.
20. Bachelet, I., A. Munitz, A. Moretta, L. Moretta, and F. Levi-Schaffer. 2005. The inhibitory receptor IRp60 (CD300a) is expressed and functional on human mast cells. *J. Immunol.* 175: 7989–7895.
21. Okoshi, Y., S. Tahara-Hanaoka, C. Nakahashi, S. Honda, A. Miyamoto, H. Kojima, T. Nagasawa, K. Shibuya, and A. Shibuya. 2005. Requirement of the tyrosines at residues 258 and 270 of MAIR-I in inhibitory effect on degranulation from basophilic leukemia RBL-2H3. *Int. Immunol.* 17: 65–72.
22. Sidorenko, S. P., and E. A. Clark. 2003. The dual-function CD150 receptor subfamily: the viral attraction. *Nat. Immunol.* 4: 19–24.
23. Chemnitz, J. M., R. V. Parry, K. E. Nichols, C. H. June, and J. L. Riley. 2004. SHP-1 and SHP-2 associate with immunoreceptor tyrosine-based switch motif of programmed death 1 upon primary human T cell stimulation, but only receptor ligation prevents T cell activation. *J. Immunol.* 173: 945–954.
24. Alvarez-Errico, D., H. Aguilar, F. Kitzig, T. Brckalo, J. Sayós, and M. López-Botet. 2004. IREM-1 is a novel inhibitory receptor expressed by myeloid cells. *Eur. J. Immunol.* 34: 3690–3701.
25. Alvarez-Errico, D., J. Sayós, and M. López-Botet. 2007. The IREM-1 (CD300f) inhibitory receptor associates with the p85α subunit of phosphoinositide 3-kinase. *J. Immunol.* 178: 808–816.
26. Takai, T., M. Li, D. Sylvestre, R. Clynes, and J. V. Ravetch. 1994. FcR γ chain deletion results in pleiotrophic effector cell defects. *Cell* 76: 519–529.
27. Colonna, M. 2003. TREMs in the immune system and beyond. *Nat. Rev. Immunol.* 3: 445–453.
28. Humphrey, M. B., L. L. Lanier, and M. C. Nakamura. 2005. Role of ITAM-containing adapter proteins and their receptors in the immune system and bone. *Immunol. Rev.* 208: 50–65.
29. Underhill, D. M., and H. S. Goodridge. 2007. The many faces of ITAMs. *Treands Immunol.* 28: 66–73.
30. Pinheiro da Silva, F., M. Aloulou, M. Benhamou, and R. C. Monteiro. 2008. Inhibitory ITAMs: a matter of life and death. *Trends Immunol.* 29: 366–373.
31. Hamerman, J. A., N. K. Tchao, C. A. Lowell, and L. L. Lanier. 2005. Enhanced Toll-like receptor responses in the absence of signaling adaptor DAP12. *Nat. Immunol.* 6: 579–586.
32. Turnbull, I. R., J. E. McDunn, T. Takai, R. R. Townsend, J. P. Cobb, and M. Colonna. 2005. DAP12 (KARAP) amplifies inflammation and increases mortality from endotoxemia and septic peritonitis. *J. Exp. Med.* 202: 363–369.
33. Takaki, R., S. R. Watson, and L. L. Lanier. 2006. DAP12: an adapter protein with dual functionality. *Immunol. Rev.* 214: 118–129.
34. Turnbull, I. R., and M. Colonna. 2007. Activating and inhibitory functions of DAP12. *Nat. Rev. Immunol.* 7: 155–161.
35. Hamerman, J. A., J. R. Jarjoura, M. B. Humphrey, M. C. Nakamura, W. E. Seaman, and L. L. Lanier. 2006. Cutting edge: inhibition of TLR and FcR responses in macrophages by triggering receptor expressed on myeloid cells (TREM)-2 and DAP12. *J. Immunol.* 177: 2051–2055.

36. Turnbull, I. R., S. Gilfillan, M. Cella, T. Aoshi, M. Miller, L. Piccio, M. Hernandez, and M. Colonna. 2006. Cutting edge: TREM-2 attenuates macrophage activation. *J. Immunol.* 177: 3520–3254.
37. Pasquier, B., P. Launay, Y. Kanamaru, I. C. Moura, S. Pfirsch, C. Ruffié, D. Hénin, M. Benhamou, M. Pretolani, U. Blank, et al. 2005. Identification of FcαRI as an inhibitory receptor that controls inflammation: dual role of FcRγ ITAM. *Immunity* 22: 31–42.
38. Wee, J. L., and D. E. Jackson. 2005. The Ig-ITIM superfamily member PECAM-1 regulates the "outside-in" signaling properties of integrin $\alpha_{IIb}\beta_3$ in platelets. *Blood* 106: 3816–3823.
39. Roncagalli, R., J. E. Taylor, S. Zhang, X. Shi, R. Chen, M. E. Cruz-Munoz, L. Yin, S. Latour, and A. Veillette. 2005. Negative regulation of natural killer cell function by EAT-2, a SAP-related adaptor. *Nat. Immunol.* 10: 1002–1010.
40. Kikuchi-Maki, A., S. Yusa, T. L. Catina, and K. S. Campbell. 2003. KIR2DL4 is an IL-2-regulated NK cell receptor that exhibits limited expression in humans but triggers strong IFN-γ production. *J. Immunol.* 171: 3415–3425.
41. Kitaura, J., J. Song, M. Tsai, K. Asai, M. Maeda-Yamamoto, A. Mocsai, Y. Kawakami, F. L. Liu, C. A. Lowell, B. G. Barisas, et al. 2003. Evidence that IgE molecules mediate a spectrum of effects on mast cell survival and activation via aggregation of the FcεRI. *Proc. Natl. Acad. Sci. USA* 100: 12911–12916.
42. Kawakami, T., and J. Kitaura. 2005. Mast cell survival and activation by IgE in the absence of antigen: a consideration of the biologic mechanisms and relevance. *J. Immunol.* 175: 4167–4173.
43. Supajatura, V., H. Ushio, A. Nakao, K. Okumura, C. Ra, and H. Ogawa. 2001. Protective roles of mast cells against enterobacterial infection are mediated by Toll-like receptor 4. *J. Immunol.* 167: 2250–2256.
44. Malaviya, R., T. Ikeda, E. Ross, and S. N. Abraham. 1996. Mast cell modulation of neutrophil influx and bacterial clearance at sites of infection through TNF-α. *Nature* 381: 77–80.
45. Echtenacher, B., D. N. Mannel, and L. Hultner. 1996. Critical protective role of mast cells in a model of acute septic peritonitis. *Nature* 381: 75–77.
46. Barclay, A. N., and D. Hatherley. 2008. The counterbalance theory for evolution and function of paired receptors. *Immunity* 29: 675–678.

Enhanced expression of *p210BCR/ABL* and aberrant expression of *Zfp423/ZNF423* induce blast crisis of chronic myelogenous leukemia

Kazuko Miyazaki,[1] Norimasa Yamasaki,[1] Hideaki Oda,[2] Takeshi Kuwata,[3] Yohei Kanno,[4] Masaki Miyazaki,[5] Yukiko Komeno,[6] Jiro Kitaura,[6] Zen-ichiro Honda,[7] Søren Warming,[8] Nancy A. Jenkins,[9] Neal G. Copeland,[9] Toshio Kitamura,[6] Takuro Nakamura,[4] and Hiroaki Honda[1]

[1]Department of Developmental Biology, Research Institute of Radiation Biology and Medicine, Hiroshima University, Hiroshima, Japan; [2]Department of Pathology, Tokyo Women's Medical University, Tokyo, Japan; [3]Pathology Section, Clinical Laboratory Division, National Cancer Center Hospital East, Chiba, Japan; [4]Division of Carcinogenesis, The Cancer Institute of Japanese Foundation for Cancer Research, Tokyo, Japan; [5]Department of Immunology, Graduate School of Biomedical Sciences, Hiroshima University, Hiroshima, Japan; [6]Division of Cellular Therapy, The Institute of Medical Science, University of Tokyo, Tokyo, Japan; [7]Department of Allergy and Rheumatology, Graduate School of Medicine, University of Tokyo, Tokyo, Japan; [8]Department of Molecular Biology, Genentech, South San Francisco, CA; and [9]Cancer Genetics Laboratory, Institute of Molecular and Cell Biology, Singapore

Chronic myelogenous leukemia (CML) is a hematopoietic disorder originating from *p210BCR/ABL*-transformed stem cells, which begins as indolent chronic phase (CP) but progresses into fatal blast crisis (BC). To investigate molecular mechanism(s) underlying disease evolution, CML-exhibiting *p210BCR/ABL* transgenic mice were crossed with BXH2 mice that transmit a replication-competent retrovirus. Whereas nontransgenic mice in the BXH2 background exclusively developed acute myeloid leukemia, *p210BCR/ABL* transgenic littermates developed nonmyeloid leukemias, in which inverse polymerase chain reaction detected 2 common viral integration sites (CISs). Interestingly, one CIS was transgene's own promoter, which up-regulated *p210BCR/ABL* expression. The other was the 5′ noncoding region of a transcription factor, *Zfp423*, which induced aberrant *Zfp423* expression. The cooperative activities of *Zfp423* and *p210BCR/ABL* were demonstrated as follows: (1) introduction of *Zfp423* in *p210BCR/ABL* transgenic bone marrow (BM) cells increased colony-forming ability, (2) suppression of *ZNF423* (human homologue of *Zfp423*) in *ZNF423*-expressing, *p210BCR/ABL*-positive hematopoietic cells retarded cell growth, (3) mice that received a transplant of BM cells transduced with *Zfp423* and *p210BCR/ABL* developed acute leukemia, and (4) expression of *ZNF423* was found in human *BCR/ABL*-positive cell lines and CML BC samples. These results demonstrate that enhanced expression of *p210BCR/ABL* and deregulated expression of *Zfp423/ZNF423* contribute to CML BC. (Blood. 2009;113: 4702-4710)

Introduction

Chronic myelogenous leukemia (CML) is a hematopoietic disorder of multipotential stem cells, which exhibits excessive proliferation of immature and mature myeloid cells.[1,2] The cytogenetic hallmark of CML is the Ph chromosome, created by t(9;22)(q34;q11),[3] where the amino-terminal *BCR* gene on chromosome 22 is fused to most of the *ABL* proto-oncogene on chromosome 9, thereby creating an 8.5-kb *BCR/ABL* chimeric mRNA encoding a 210-kDa hybrid protein (p210BCR/ABL).[4-6] p210BCR/ABL possesses a much higher kinase activity in comparison with the normal 145-kDa c-ABL,[7] which is believed to play a critical role in the pathogenesis of the disease.

The clinical course of CML is characterized by hematologically and temporally distinct stages.[1,2] In the initial stage, called chronic phase (CP), the disease is indolent and the leukemic cells retain an ability to differentiate into mature granulocytes. After several years' duration of the chronic phase, however, the disease inevitably accelerates and ultimately progresses to the terminal fatal stage, called blast crisis (BC), which involves aggressive proliferation of immature blast cells. The frequent appearances of additional chromosomal abnormalities in the blast phase strongly suggest that superimposed genetic events would account for the disease evolution,[8] but the underlying molecular mechanism(s) has remained largely unknown.

To understand the complex processes involved in the clinical course of human CML, it is necessary to develop animal models that express *p210BCR/ABL* and recapitulate the clinical features of the disease. Major attempts have been focused on bone marrow transplantation (BMT) experiments. Mice that have been lethally irradiated and received a transplant of bone marrow (BM) cells infected with *p210BCR/ABL*-expressing retroviruses exhibited a CML-like myeloproliferative disorder.[9-11] On the other hand, generation of transgenic mice expressing *p210BCR/ABL* under various promoters also provides useful models.[12-17] We generated *p210BCR/ABL* transgenic mice using the promoter from the mouse *TEC* gene, a gene encoding protein-tyrosine kinase preferentially expressed in hematopoietic progenitor cells.[18,19] Although the founder mouse died of T-cell acute lymphoblastic leukemia (ALL) with a short latency, transgenic offspring reproducibly exhibited a myeloproliferative disorder after a long latency period.[14] Peripheral blood smear showed remarkable myeloid hyperplasia with maturation, the BM was hypercellular with a predominance of myeloid cells at various stages of differentiation, and the spleen was enlarged with proliferation and expansion of myeloid cells.[14] These

Submitted May 3, 2007; accepted January 29, 2009. Prepublished online as *Blood* First Edition paper, February 20, 2009; DOI 10.1182/blood-2007-05-088724.

The online version of this article contains a data supplement.

The publication costs of this article were defrayed in part by page charge payment. Therefore, and solely to indicate this fact, this article is hereby marked "advertisement" in accordance with 18 USC section 1734.

pictures represent cardinal features of human CML, allowing us to consider these transgenic mice an animal model for CML.

To examine whether this transgenic model is applicable for investigating pathogenic processes from CP to BC of CML, we crossed *p210BCR/ABL* transgenic mice with mice heterozygous for *p53*, a gene frequently inactivated in CML BC, and generated mice transgenic for *p210BCR/ABL* and heterozygous for *p53*.[20] Interestingly, *p210BCR/ABL* transgenic, *p53* heterozygous mice died of acute leukemia with a short latency, and the analysis of *p53* status revealed that the residual normal *p53* allele was frequently and preferentially lost in the tumor tissues.[20] In addition, we crossed *p210BCR/ABL* transgenic mice with *Dok-1/Dok-2* knockout mice and showed that the absence of Dok-1 and Dok-2 accelerated the disease phenotype and caused BC, defining the role of Dok-1 and Dok-2 in tumor suppression.[21] Based on these results, our transgenic mice can be regarded as a useful model for investigating molecular mechanism(s) underlying the progression from CP to BC of human CML.

In this report, to identify genes whose altered expression causes CML BC, *p210BCR/ABL* transgenic mice were subjected to retroviral insertional mutagenesis, by backcrossing to BXH2 mice, a recombinant inbred mouse strain that develop myeloid leukemia mainly due to a horizontally transmitted replication-competent retrovirus and intrinsic myeloid tropism induced by a mutation in the *Icsbp1/Irf8* locus.[22-24]

Methods

Mice

p210BCR/ABL transgenic mice were generated as described.[14] To allow for retroviral insertional mutagenesis, *p210BCR/ABL* transgenic males were backcrossed 4 generations to BXH2 females, because the ecotropic retrovirus in the BXH2 strain is transmitted to the progeny through the milk. Genotyping of the mice was carried out as described.[14] All the mice used in this study were kept according to the guidelines of the Institute of Laboratory Animal Science, Hiroshima University, and all murine studies were approved by the animal care committee at the Japanese Foundation for Cancer Research.

Hematologic and pathologic analyses

Peripheral blood counts were routinely examined. Smears and stamp specimens of leukemic tissues were stained with Wright-Giemsa (WG). Tissues from dead or moribund animals were fixed in 10% buffered formaldehyde and examined by light microscopy. All organs were examined grossly and representative slices were prepared for hematoxylin-eosin staining.

Southern and Northern blot analyses

To detect gene rearrangements, genomic DNAs were digested with appropriate restriction enzymes and blotted with a genomic fragment adjacent to the integration site. For transgene promoter, a *BglI-SmaI* fragment in the promoter region was used as a probe, and for *Zfp423*, a genomic fragment generated by polymerase chain reaction (PCR) (primer sequences are 5′-GTGCGCACGTTTGTGAGGAGCTATA-3′ and 5′-CCAGCTATTCTGTCCAGGAGCAAGA-3′), which corresponds to a part of the first intron, was used as a probe. To detect RNA expression, total RNA extracted using TRIzol (Invitrogen, Carlsbad, CA) or mRNA purified using Oligo-Tex (Takara Bio, Tokyo, Japan) was blotted with *p210BCR/ABL* cDNA, *Zfp423* cDNA, or a part of coding region of *ZNF423* cDNA generated by genomic PCR (primer sequences are 5′-CAACCAGAAACACAAGTGCCCCATG-3′ and 5′-GTTGCAGTGGAAGGCAGAGATGTTG-3′).

RT-PCR

RNA was extracted using TRI zol. Reverse-transcription (RT)–PCR was performed as described (primer sequences are 5′-GAATGTCATCGTCCACTCAGCC-3′ and 5′-GGCCACAAAATCATACAGTGCA-3′ for *p210BCR/ABL*, 5′-GAGGATACCCCTACGACGTG-3′ and 5′-GACTTGTCACGCTGTTCCTGTC-3′ for *Zfp423*, and 5′-GGCATCAACCACGAGTGTAAGC-3′ and 5′-CTTCTGCGGAGAGGTGTCCTGT-3′ for *ZNF423*).[25]

Western blot analysis

Proteins extraction and Western blot were performed as described.[14]

Flow cytometric analysis

Cells were stained with monoclonal antibodies and second reagents. FITC-, PE-, and biotin-labeled monoclonal antibodies were purchased from BD PharMingen (San Diego, CA; Thy-1.2, CD19, CD45R/B220, Mac-1, Gr-1, and CD3) or from eBioscience (San Diego, CA; CD43, IgM, BP-1, and CD20). Biotinylated antibodies were revealed with streptavidin-APC (BD PharMingen). Clone 2.4G2 anti-CD32:CD16 was used to block Fc receptors. Fluorescence-activated cell sorter (FACS) analysis was performed on a FACSCalibur flow cytometer (Becton Dickinson, Franklin Lakes, NJ), and the data were analyzed with FlowJo software (TreeStar, Ashland, OR).

Identification of retroviral integration sites

Genomic DNAs were digested with restriction enzymes, self-ligated, and subjected to inverse PCR as described,[22] except that the CUA and CAU repeats were deleted from the secondary PCR primers. The position mapping on the mouse chromosome was done by BLAST searching using the University of Colombo School of Computing (UCSC) Genome Bioinformatics database (http://genome.ucsc.edu/)[26] and the definition of a common integration site (CIS) was the same as in the mouse retrovirus tagged cancer gene database (RTCGD; http://rtcgd.abcc.ncifcrf.gov/).[23,27]

Retrovirus-mediated gene transfer, colony formation assay, and bone marrow transplantation

Retroviral preparation and retrovirus-mediated gene transfer were performed as described.[28] For colony assay, BM cells of 5-fluorouracil (5FU)–treated transgenic or nontransgenic littermates were cultured in αMEM plus 20% FCS supplemented with 10 ng/mL IL-6, 10 ng/mL IL-3, and 100 ng/mL SCF (R&D Systems, Minneapolis, MN). Retrovirus was generated using plat-E cells[29] and added into the medium containing BM cells with 6 mg/mL polybrene (Sigma-Aldrich, St Louis, MO), and retrovirus-infected BM cells were subjected to B-cell colony assay using MethoCult M3630 (StemCell Technologies, Vancouver, BC) that contains rhIL7. After 7 to 12 days' incubation, green colony numbers were counted under a fluorescent microscope.

For BM transplantation, BM cells extracted from 5FU-untreated Balb/c mice were cultured for 24 hours in IMDM plus 15% FCS supplemented with 10 ng/mL IL-6, 10 ng/mL IL-3, 100 ng/mL SCF, and 10 ng/mL IL-7 (R&D Systems). Retrovirus infection and BM transplantation were performed as described.[30]

Retrovirus-mediated transduction of shRNA for *ZNF423*

Two short hairpin RNA (shRNA) target sequences for *ZNF423* (5′-GACATACCAGTGCATCAAG-3′ for *shRNA*-1 and 5′-CTGTAAGTTCTGCAGCAAG-3′ for *shRNA*-2) were chosen according to the siRNA Hairpin Oligonucleotide Sequence Designer (Clontech, Mountain View, CA). Annealed double-strand oligonucleotides were subcloned into RNA-ready pSIREN-retroQ retroviral expression vector (Clontech). Human hematopoietic cells were first transduced with ecotropic retrovirus receptor (EcoRVR) to render these cells competent for ecotropic retrovirus infection.[31] Plat-E cells were then transfected with a pSIREN-retroQ vector harboring *shRNA* and the culture supernatant was used for infecting the ecotropic retrovirus to EcoRVR-expressing cells using Viro Mag (OZ Biosciences, Marseille, France). These procedures routinely yielded a high

infection efficiency (~ 60%) as judged by GFP fluorescence (not shown). Infected cells were selected with puromycin (0.4 mg/mL) for 2 weeks, subsequently cultured in puromycin-free medium for at least another 2 weeks, and subjected to Northern blot and cell proliferation assay.

Cell proliferation assay

On day 1, 10^5 cells of the parental and *shRNA*-transduced sublines were plated in a 10-cm^2 dish and cultured in RPMI plus 10% FCS. Cell numbers were counted on day 3 and day 5.

Cell lines and patient samples

Ph-positive and Ph-negative human hematopoietic cell lines were kindly provided by Drs Hiroya Aso (Hiroshima, Japan) and Toshiya Inaba (Hiroshima, Japan). Patient samples were taken after informed consent was obtained in accordance with the Declaration of Helsinki and approval from the institutional review board at Hiroshima University was granted.[32] Diagnosis of CML CP or CML BC (myeloid or B-lymphoid lineage) was performed based on morphologic, cytogenetic, immunophenotypic, and molecular analyses.

Results

Acute leukemias in *p210BCR/ABL* transgenic mice on a BXH2 background

To identify gene(s) whose alteration by retrovirus insertion contributes to blast crisis of CML, *p210BCR/ABL* transgenic mice were backcrossed to BXH2 mice that contain and transmit a replication-competent retrovirus. *p210BCR/ABL* transgenic and wild-type (nontransgenic) littermates from the N4 BXH2 backcross generation were used for this study (designated as p210BCR/ABL/BXH2 and WT/BXH2, respectively).

WT/BXH2 mice began to develop acute leukemia at 6 months after birth (Figure 1A thin continuous line). Macroscopically, the leukemic mice exhibited hepatosplenomegaly and lymph node (LN) swelling, which were occasionally associated with thymic enlargement. Pathologic analysis showed that leukemic cells having morphology of myeloblasts proliferated in the peripheral blood and infiltrated into the liver, spleen, LNs, and other tissues (data not shown). Flow cytometric analysis of the leukemic tissues showed that the blast cells were exclusively positive for Mac-1 and Gr-1 but negative for Thy1.2 and CD19, indicating that they all were of myeloid origin (data not shown).

In contrast to the WT/BXH2 mice, several p210BCR/ABL/BXH2 mice (named as nos. 30, 1, 17, 5, 18, and 23; Figure 1A thick continuous line) developed nonmyeloid leukemias with a shorter latency. Among them, 4 mice (nos. 30, 17, 18, and 23) displayed splenomegaly and LN swelling but did not show apparent hepatomegaly. The other 2 mice (nos. 1 and 5) exhibited massive thymic enlargement with pleural effusion and splenomegaly. Pathologic analysis showed that leukemic cells having morphology of lymphoblasts were evident in the peripheral blood and infiltration of the blast cells was observed in the LNs, liver, and other tissues examined (Figure 1B and not shown). Flow cytometric analysis revealed that the leukemic cells of the former 4 mice (nos. 30, 17, 18, and 23) were positive for CD19 but negative for Thy1.2, Mac-1, and Gr-1, and those of the latter 2 mice (nos. 1 and 5) were positive for Thy1.2 but negative for CD19, Mac-1, and Gr-1, indicating that they were of B-lymphoid and T-lymphoid origins, respectively (Figure 1C and not shown). Three $CD19^+$ samples (nos. 17, 18, and 30) were further analyzed with antibodies against CD20, B220, BP-1, CD43, and IgM to investigate the differentiation stages (pro-B, pre-B, or mature B). As shown in Figure S1 (available on the *Blood* website; see the Supplemental Materials link at the top of the online article), all the samples were positive for CD20, B220, BP-1, and CD43 but negative for IgM, indicating that they were pre–B-cell leukemias.

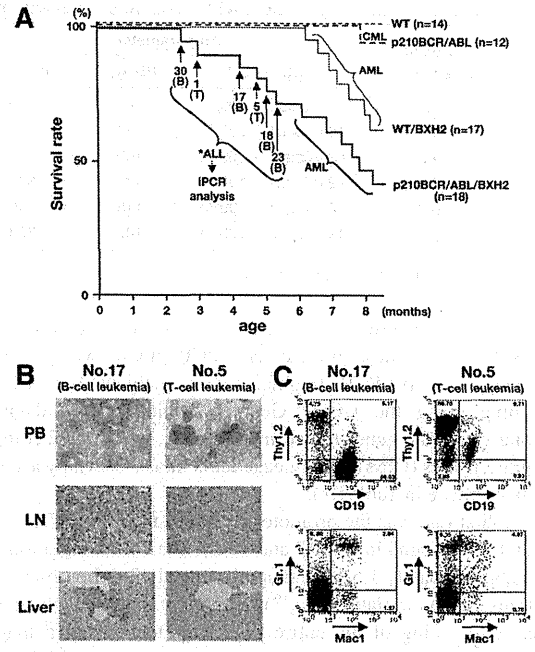

Figure 1. Survival curves and pathologic and flow cytometric analyses of leukemic mice. (A) Survival curves of the mice. The survival curves of WT/BXH2 and p210BCR/ABL/BXH2 are shown by thin and thick continuous lines, respectively, whereas those of BXH2-nonbackcrossed WT and p210BCR/ABL are shown by thin and thick dotted lines, respectively. As for the 6 p210BCR/ABL/BXH2 animals that died in a short latency and exhibited nonmyeloid phenotypes (nos. 30, 1, 17, 5, 18, and 23), the death points are indicated by → and the immunophenotypes of the disease are shown in the parentheses. T indicates T-cell leukemia; and B, B-cell leukemia. (B) Pathologic analysis of the leukemic mice. WG-stained peripheral blood smears (PB) and HE-stained lymph node (LN) and liver slices of a representative mouse for B-cell leukemia (no. 17) or T-cell leukemia (no. 5) are shown. PB smears show proliferation of blast cells and LN specimen shows the destruction of the basal structure by blast cell infiltration. In the liver, blast cells are observed around the vessel and in the sinusoids. (C) Flow cytometric analysis of mice that developed B-cell or T-cell leukemia. Blast cells of no. 17 were positive for CD19 but negative for Thy1.2, Mac-1, and Gr-1 and those of no. 5 were positive for Thy1.2 but negative for CD19, Mac-1, and Gr-1, indicating that they were of B- and T-lymphoid origins, respectively. The percentages of positive cells in each quadrant are shown.

The characteristics of the 6 p210BCR/ABL/BXH2 leukemic mice with an early disease onset are summarized in Table 1. As for the leukemias developed in the remaining p210BCR/ABL/BXH2 mice after 6 months of age, macroscopic appearances and the results of flow cytometric analysis were indistinguishable from those of the WT/BXH2 mice (data not shown). During the observation period, no mice developed hematologic disease in BXH2-nonbackcrossed WT mice and one mouse died of CML in BXH2-nonbackcrossed *p210BCR/ABL* transgenic mice (Figure 1A thin and thick dotted lines, respectively).

Enhanced expression of *p210BCR/ABL* and aberrant expression of *Zfp423* in the leukemic tissues with B-cell phenotype

We focused on the 6 p210BCR/ABL/BXH2 mice that developed nonmyeloid leukemias in a shortened period, because diseases in these mice would not be only due to the BXH2 background-derived intrinsic mechanism but caused by cooperation of *p210BCR/ABL*

Table 1. Characteristics of p210BCR/ABL/BHX2 mice with lymphoid leukemias

Mouse no.	Age at disease, mo	PB parameters			Macroscopic tumor sites	Surface markers	Diagnosis
		WBC, $\times 10^{9}$/L	Hb, g/L	Plt, $\times 10^{9}$/L			
30	2.6	11.2 (blast ~ 70%)	140	452	Spl, LN	Thy1.2$^-$, CD19$^+$, Gr.1$^-$, Mac1$^-$	B-cell leukemia
1	3.0	10.0 (blast ~ 60%)	124	238	Thy, Spl	Thy1.2$^+$, CD19$^-$, Gr.1$^-$, Mac1$^-$	T-cell leukemia
17	4.2	82.4 (blast ~ 100%)	109	525	Spl, LN	Thy1.2$^+$, CD19$^-$, Gr.1$^-$, Mac1$^-$	B-cell leukemia
5	4.8	22.0 (blast ~ 100%)	123	339	Thy, Spl, LN	Thy1.2$^-$, CD19$^+$, Gr.1$^-$, Mac1$^-$	T-cell leukemia
18	5.2	68.0 (blast ~ 100%)	118	345	Spl, LN	Thy1.2$^-$, CD19$^+$, Gr.1$^-$, Mac1$^-$	B-cell leukemia
23	5.4	19.8 (blast ~ 100%)	107	338	Spl, LN	Thy1.2$^-$, CD19$^+$, Gr.1$^-$, Mac1$^-$	B-cell leukemia

Spl indicates spleen; LN, lymph node; and Thy, thymus.

with retrovirus-inserted altered gene expression. To identify virus-affected genes in these mice, inverse PCR (iPCR) was performed and sequences of PCR fragments were subjected to BLAST searching using the UCSC Genome Bioinformatics database. Among candidate genes (listed in Table S1), we found 2 common integration sites (CISs) in B-lineage leukemias (shown by asterisks and in boldface in Table S1).

The first one was the promoter region of the mouse *TEC* gene. This CIS was found in nos. 17 and 30 and the viral integration sites were approximately 1.5-kb and approximately 200-bp upstream of the transcription initiation site,[19] respectively. Interestingly, in both cases, sequencing of the entire PCR fragment revealed that the mouse *TEC* promoter sequences were interrupted at +22 from the transcription initiation site and followed by human *BCR/ABL* cDNA. This result indicated that the integration sites were not in the endogenous mouse *TEC* gene but in the promoter region of the transgene itself. Another CIS observed in nos. 18 and 23 was in the noncoding region of the first exon of mouse *Zfp423* (*Zinc finger protein 423,* also known as *Early B-cell factor-associated zinc-finger protein, Ebfaz*) gene.[33] In these cases, the retroviruses were integrated almost in the same position, approximately 100-bp upstream of the translational initiation ATG.[33] The schematic models of the integration sites are shown in Figure 2A.

To confirm that these CISs were major integration sites in the leukemic samples, Southern blot was performed using a genomic DNA fragment adjacent to the integration site. DNA extracted from a spleen of a BXH2-nonbackcrossed *p210BCR/ABL* transgenic mouse was used as a negative control. As shown in Figure 2B, a rearranged band is evident in each sample (indicated by an arrowhead in Figure 2B), indicating that tumor cells with the CISs were predominant in the related tumors and were clonal in origin. The clonality and B-cell commitment of the leukemic cells in these mice (nos. 17, 30, 18, and 23) were further demonstrated by Southern blot using a mouse JH probe (Figure S2).

To investigate the alteration in gene expression of *p210BCR/ABL* and *Zfp423* by virus integration, RNAs extracted from tumor tissues of the 4 leukemic mice were blotted with *p210BCR/ABL* cDNA or mouse *Zfp423* cDNA. RNA extracted from a spleen of a BXH2-nonbackcrossed *p210BCR/ABL* transgenic mouse was used as control. The results are shown in upper panels of Figure 2C.

As for *p210BCR/ABL,* it is not surprising that the *p210BCR/ABL* message was not detected in the control transgenic mouse spleen (Figure 2C top left panel, "C"), because our previous data showed that the basal transgene expression was quite low, probably due to the nature of the promoter used (Honda et al[14] and data not shown). In contrast, a clear *p210BCR/ABL* message was evident in the tumors of nos. 17 and 30 (~ 7 kb, Figure 2C top left top panel, arrow). The quantitative *p210BCR/ABL* mRNA expression in these samples is shown in Figure S3. As expected from the result of the Northern blot (Figure 2C top left panel), the *p210BCR/ABL* mRNA in the control transgenic spleen was quite low and was significantly enhanced by the transgene integration (nos. 17 and 30). The enhanced expression of p210BCR/ABL at the protein level was confirmed by Western blot using an anti-ABL antibody (Figure 2C bottom left panel).

As for *Zfp423,* no clear message was observed in the control transgenic spleen (Figure 2C top right panel, "C"), which is in accordance with our previous report showing that *Zfp423* message was barely detectable in the spleen when using polyA$^+$ RNA.[34] In contrast, in nos. 18 and 23, an enhanced expression of the *Zfp423* message was observed (~ 6 kb, Figure 2C top right panel, arrow). These results indicated that the retrovirus integrations up-regulated *p210BCR/ABL* expression and induced aberrant *Zfp423* expression.

Expression of *Zfp423* in transgenic BM cells enhanced B-cell colony-forming ability, and suppression of *ZNF423* in *ZNF423*-expressing, *p210BCR/ABL*-positive CML BC cells retarded cell growth

We next investigated the effect of up-regulation and down-regulation of *Zfp423* on the proliferative ability of *p210BCR/ABL*-positive cells. We first examined whether introduction of *Zfp423* confers a growth advantage to transgenic BM cells by a colony formation assay. BM cells purified from wild-type (WT) or *p210BCR/ABL* transgenic mice were infected with control *pMysIG* or *Flag-HA*–tagged *Zfp423 (FHZfp423)*–expressing *pMysIG (pMysIG/FHZfp423)* retrovirus, and the infected cells were cultured in methylcellulose-based media (Figure 3A). Because mice with *Zfp423* activation (nos. 18 and 23) developed B-lineage leukemia, the virus-infected cells were subjected to a B-cell colony assay, and as the retrovirus vector contains *GFP* as a detection marker, colonies with green fluorescence were counted.

The results are shown in Figure 3B. No obvious difference in the colony numbers was found between control *pMysIG* virus-infected WT (WT+control) and *p210BCR/ABL* transgenic (p210BCR/ABL+control) BM cells. This result indicates that the basal *p210BCR/ABL* expression in this transgenic system does not affect the proliferative ability of B cells, probably due to the nature of the promoter used, and is in accordance with our observation that the *p210BCR/ABL* transgenic mice have not developed B-cell disease so far.[14] *pMysIG/FHZfp423*-infected WT BM cells (WT+FHZfp423) showed a slight increase in the colony number in this system. In contrast, *pMysIG/FHZfp423*-infected *p210BCR/ABL* transgenic BM cells (p210BCR/ABL+FHZfp423) generated a significantly increased number of colonies.

We next tried to down-regulate endogenous *ZNF423* (the human homologue of *Zfp423*) by RNA interference and examined its effect on the growth rate. We designed 2 short hairpin RNAs targeted to *ZNF423* mRNA (*shRNA*-1 and *shRNA*-2) and introduced them into BV-173, a *p210BCR/ABL*-positive and *ZNF423*-expressing human hematopoietic cell line (see Figure 5A). As shown in Figure 3C, introduction of *shRNA*-1 effectively decreased

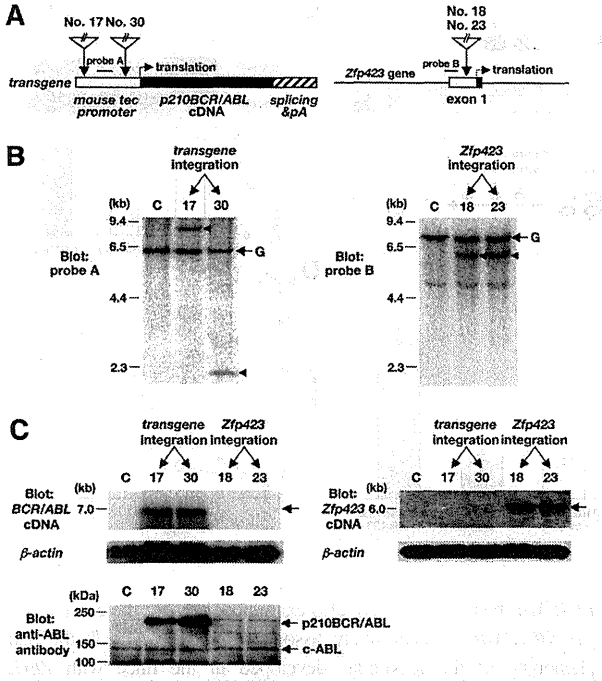

Figure 2. Retrovirus integration sites, genomic rearrangements, and altered gene expressions in mice with B-cell leukemia. (A) Schematic models of retrovirus integration sites. The retrovirus integration sites are indicated by vertical arrows. The left panel illustrates the transgene structure, where the mouse *TEC* promoter, *p210BCR/ABL* cDNA, and polyA and splicing signals are shown by dotted, filled, and shaded boxes, respectively. In mice nos. 17 and 30, retroviruses were integrated approximately 1.5-kb and approximately 200-bp upstream of the transcriptional initiation site, respectively. In the right panel, the noncoding and coding regions of *Zfp423* exon 1 are shown by blank and filled boxes, respectively. In mice nos. 18 and 23, the viral integration occurred almost in the same site, approximately 100-bp upstream of the translational initiation site. The positions of probes used for Southern blots are also shown. (B) Southern blots to confirm the CISs as major integration sites. Genomic DNAs extracted from the spleen of a control transgenic mouse (C) and tumor tissues of the diseased mice (nos. 17, 30, 18, and 23) were digested with *Bam*HI and blotted with a DNA fragment adjacent to the integration site. Probe A (A) was used for transgene rearrangement (nos. 17 and 30, left panel) and probe B was used for *Zfp423* gene rearrangement (nos. 18 and 23, right panel). The positions of germline (G) and rearranged bands are indicated by → and ◀, respectively. Molecular markers are shown on the left. (C) Enhanced expression of *p210BCR/ABL* in mice nos. 17 and 30 and up-regulated expression of *Zfp423* in mice nos. 18 and 23. For detecting *p210BCR/ABL* message, 20 μg total RNAs extracted from the spleen of a control *p210BCR/ABL* transgenic mouse (C) and tumor tissues of the diseased mice (nos. 17, 30, 18, and 23) were blotted with *p210BCR/ABL* cDNA (top left panel) and for detecting *Zfp423* message, 3 μg mRNAs from the same tissues were blotted with a part of *Zfp423* cDNA (top right panel). The result of β-*actin* hybridization is shown as an internal control. Molecular markers are shown on the left and the positions of *p210BCR/ABL* and *Zfp423* messages are indicated by →. Enhanced expression of p210BCR/ABL protein in mice nos. 17 and 30 was detected by blotting the proteins extracted from the same tissues with an anti-ABL antibody (bottom left panel). Protein markers are shown on the left and the positions of p210BCR/ABL and c-ABL (145 kDa) are indicated by →.

ZNF423 mRNA to approximately 40% of that in the parental cells, whereas *shRNA*-2 was less effective. Concurrently, as shown Figure 3D, BV-173 cells transduced with *shRNA*-1 displayed a significantly reduced growth rate, whereas cells expressing *shRNA*-2 showed only marginal growth retardation. To confirm that the *shRNA*s did not affect the growth of cells without *ZNF423* expression, the same *shRNA*s were introduced into KOPN67, a *p210BCR/ABL*-positive but *ZNF423*-nonexpressing cell line (see Figure 5A). As expected, no difference in cell growth was observed in the parental line and *shRNA*s-transduced sublines (Figure S4), confirming the specificity of the *shRNA*s on the *ZNF423*-dependent cell growth. These results indicated that *Zfp423/ZNF423* cooperated with *p210BCR/ABL* and enhanced proliferation of *p210BCR/ABL*-expressing hematopoietic cells.

Zfp423 accelerated disease onset of *p210BCR/ABL*-induced leukemia and increased incidence of B-ALL

We then investigated the in vivo cooperative activity of *Zfp423* and *p210BCR/ABL* by a BMT approach. Because *p210BCR/ABL* transgenic mice were not congenic enough for BMT, we generated *p210BCR/ABL*-expressing retrovirus and *FHZfp423*-expressing retrovirus separately, and infected them with BM cells of Balb/c mice, the strain that has been successfully used to develop CML in the BMT experiments.[10,11] And because *Zfp423*-positive leukemias (nos. 18 and 23) were of B-cell phenotype, BM cells were not pretreated with 5FU and in vitro cultures were performed using a cytokine cocktail with IL-6, IL-3, SCF, and IL-7, as previously described.[11]

BM cells infected with control retrovirus, *p210BCR/ABL*-expressing retrovirus, *FHZfp423*-expressing retrovirus, or both types of viruses were transplanted into sublethally irradiated syngeneic mice (Figure 4A). To detect *p210BCR/ABL*- and *FHZfp423*-positive cells by flow cytometry, cells expressing *p210BCR/ABL* and *FHZfp423* were labeled with *GFP* and *KO* (*Kusabira Orange*),[35] respectively (Figure 4A). The protein expression of the inserted cDNA by retrovirus infection was confirmed by Western blot (Figure S5).

The mice that underwent transplantation were continuously observed and peripheral blood parameters were routinely examined for morphologic changes by Wight-Giemsa staining and for *GFP* and/or *KO* positivities by flow cytometry. The survival rate of each group evaluated using the Kaplan-Meier test is shown in the upper panel of Figure 4B. No disease developed in the control virus-transduced mice. In addition, no hematologic abnormalities were observed in FHZfp423-transduced mice, indicating that overexpression of *Zfp423* does not possess a transforming ability on primary hematopoietic cells, which is in accordance with the result that introduction of *Zfp423* in BM cells did not apparently increase colony numbers (Figure 3B). As expected from the results of previous studies, most of the *p210BCR/ABL*-transduced mice developed CML, except 2 cases that developed acute myeloid leukemia (AML) and B-cell ALL (B-ALL, Figure 4B bottom panel, left bar). In contrast, mice transduced with both types of viruses died in a shortened period and exhibited different phenotypes. The mean survival periods of mice reconstituted with p210BCR/ABL+FHZfp423 and those reconstituted with p210BCR/ABL alone were 29.5 and 48 days, respectively (Figure 4B top panel, thick and thin continuous lines), and the difference was statistically significant ($P < .01$). In addition, compared with mice reconstituted with p210BCR/ABL, those reconstituted with p210BCR/ABL+FHZfp423 exhibited an increased incidence of B-ALL (Figure 5B bottom panel, right bar), although the difference was not statistically significant ($P = .119$), probably due to the limited sample numbers. These results demonstrated that *Zfp423* possesses a cooperative oncogenecity with *p210BCR/ABL* in vivo, which accelerated disease onset and induced a more aggressive phenotype mainly of B-cell lineage. The representative results of pathologic analyses of mice that developed CML by p210BCR/ABL and that developed B-ALL by p210BCR/ABL plus FHZfp423 are shown in Figure 4C and the results of flow cytometry of the latter are shown in Figure 4D. The expression of *p210BCR/ABL* and *Zfp423* mRNAs in tumors developed in p210BCR/ABL plus FHZfp423-transduced mice was confirmed by RT-PCR (Figure S6).

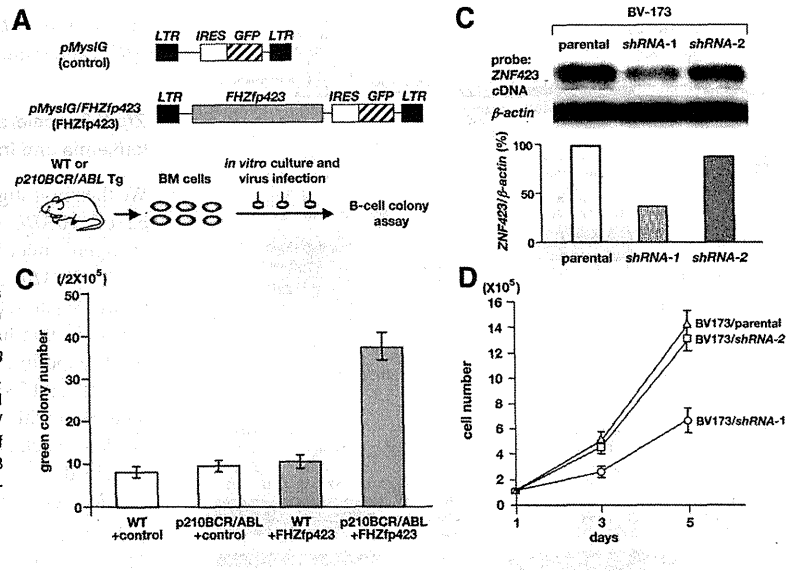

Figure 3. Effects of *Zfp423* expression on the colony formation and proliferation of *p210BCR/ABL*-expressing cells. (A) Schematic structures of the retroviruses and the illustration of the experimental procedure. BM cells were extracted from WT or *p210BCR/ABL* transgenic mice, infected with empty retrovirus (*pMyIG*, control) or *Flag-HA*–tagged *Zfp423 (FHZfp423)*–expressing retrovirus (*pMyIG*/FHZfp423, FHZfp423), and subjected to the B-cell colony assay. (B) Results of B-cell colony assay. The mean green colony number of 3 independent experiments for each group (WT+conrol, p210BCR/ABL+control, WT+FHZfp423, and p210BCR/ABL+FHZfp423) is shown with error bars. (C) Suppression of *ZNF423* expression by *shRNAs*. mRNA (5 μg) extracted from the parental BV-173 line and 2 *shRNA*-introduced sublines (*shRNA-1* and *shRNA-2*) were blotted with a part of the human *ZNF423* coding region. β-*Actin* hybridization was performed as an internal control and the relative expression ratio of *ZNF423* to β-*actin* in each cell line is shown as a vertical column. (D) Results of cell proliferation assay. Cells of the parental BV-173 line and 2 *shRNA*-introduced sublines (BV-173/*shRNA-1* and BV-173/*shRNA-2*) were plated at a density of 10^5/10 cm^2 on day 1 and cell numbers were counted on day 3 and day 5. The mean cell number of 3 independent experiments of each line is plotted with error bars.

Expression of *ZNF423* in human *BCR/ABL*-positive hematopoietic cell lines and CML BC samples

We finally investigated the clinical relevance of *ZNF423* expression in the progression from CML CP to BC using human Ph-positive hematopoietic cell lines and clinical samples. For the cell line experiment, cells expressing *p190BCR/ABL* (an alternative form of the *BCR/ABL* fusion gene) were also examined, because the expression of *p190BCR/ABL* is exclusively associated with B-ALL,[36] the same phenotype as the leukemias developed in the mice with *Zfp423* integration (nos. 18 and 23). In addition, Ph-negative B-ALL lines were included in this study to investigate the role of *ZNF423* in the development of B-cell malignancy without *BCR/ABL*.

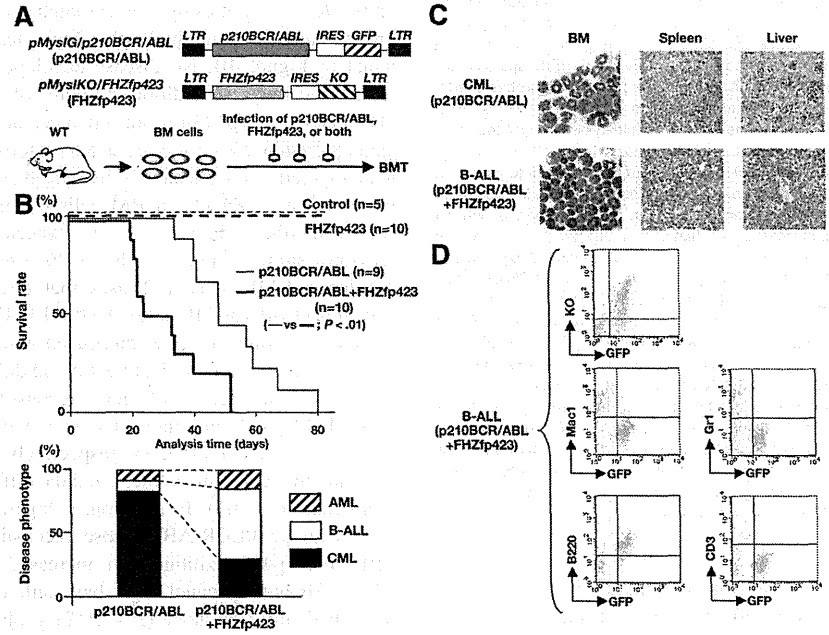

Figure 4. Survival and disease phenotype in mice that received a transplant of *p210BCR/ABL*- and/or *FHZfp423*-expressing BM cells. (A) Schematic structures of the retroviruses and the illustration of the experimental procedure. BM cells infected with *p210BCR/ABL*-expressing retrovirus (*pMyIG/p210BCR/ABL*), *FHZfp423*-expressing retrovirus (*pMyIKO/FHZfp423*), or both types of viruses were subjected to the BMT assay. KO indicates Kusabira Orange. (B) Acceleration of disease onset and altered disease phenotype by cotransduction of *Zfp423* and *p210BCR/ABL*. In the top panel, survival curves of mice reconstituted with BM cells transduced with control retrovirus (control, n = 5), *pMyIKO/FHZfp423* (FHZfp423, n = 10), *pMyIG/p210BCR/ABL* (p210BCR/ABL, n = 9), and both viruses (p210BCR/ABL+FHZfp423, n = 10) are shown as thin dotted, thick dotted, thin continuous, and thick continuous lines, respectively. In the bottom panel, the percentages of samples diagnosed as CML, B-ALL, and AML are shown by black, white, and shaded boxes, respectively. (C) Representative results of pathologic analysis of CML and B-ALL developed in mice transduced with p210BCR/ABL and p210BCR/ABL+FHZfp423, respectively. In the BM smears, proliferation of differentiated myeloid cells is observed in the CML case (top left panel), whereas monotonous proliferation of immature lymphoid tumor cells is apparent in the B-ALL case (bottom left panel). Massive infiltration of leukemic cells is shown in the spleen and liver (middle and right panels). (D) Representative results of flow cytometric analysis of B-ALL developed in mice transduced with p210BCR/ABL and FHZfp423. Leukemic cells are positive for both GFP and KO (top panel), confirming that they were originated from hematopoietic progenitor cells infected with both p210BCR/ABL and FHZfp423. GFP-positive leukemic cells showed positive staining for B220, but are negative for Mac-1, Gr-1, and CD3 (middle and bottom panels).

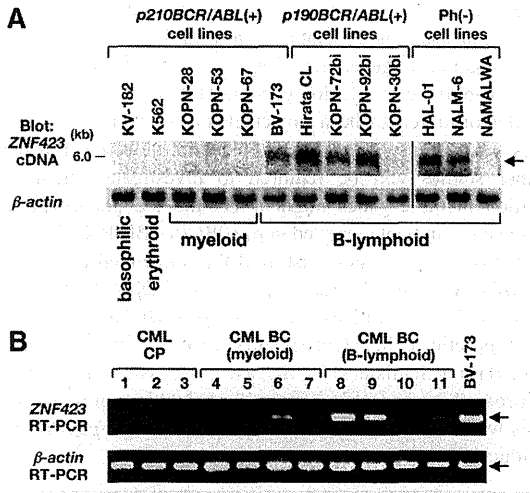

Figure 5. Expression of *ZNF423* in *BCR/ABL*-positive cell lines and in CML BC samples. (A) mRNA (3 μg) extracted from 6 *p210BCR/ABL*-positive, 4 *p190BCR/ABL*-positive, and 3 Ph-negative cell lines was blotted with a part of the human *ZNF423* coding region. β-*Actin* hybridization was performed as an internal control. The position of the *ZNF423* message is indicated by → and the immunophenotypes of the cell lines are shown at the bottom. A vertical line has been inserted to indicate a repositioned gel lane. (B) Total RNAs extracted BM samples from 3 CML CP and 8 CML BC cases (4 myeloid and 4 B-lymphoid) were subjected to RT-PCR for *ZNF423* expression. β-*Actin* RT-PCR was performed as an internal control.

mRNAs extracted from 6 *p210BCR/ABL*-positive cell lines (1 B-lymphoid, 3 myeloid, 1 erythroid, and 1 basophilic), 4 *p190BCR/ABL*-positive B-lymphoid cell lines, and 3 Ph-negative B-lymphoid cell lines were blotted with human *ZNF423* cDNA. As shown in Figure 5A, *ZNF423* mRNA expression was detected in 1 of 6 *p210BCR/ABL*-positive (BV-173), 3 of 4 *p190BCR/ABL*-positive (Hirata CL, KOPN-72bi, and KOPN-92bi), and 2 of 3 Ph-negative cell lines (HAL-01 and NALM-6), all of which were of B-cell phenotype.

We then examined *ZNF423* expression in human clinical samples diagnosed as CML CP or BC. BM samples of 3 CML CP and 4 CML BC patients (4 myeloid and 4 B-lymphoid lineages) with informed consent were subjected to RT-PCR using *ZNF423*-specific primers. BV-173 cells that express *ZNF423* (Figure 5A) were used as a control. As shown in Figure 5B, whereas no *ZNF423* expression was detected in CML CP sample (nos. 1-3), 4 of 8 CML BC samples were found to express *ZNF423,* where 1 was of myeloid (no. 6) and the other 3 were of B-lymphoid (nos. 8, 9, and 11) phenotypes. These results strongly indicated that aberrant expression of *ZNF423* clinically contributes to the malignant transformation of *BCR/ABL*-positive cells and to the progression to CML BC, mainly of B-cell lineage.

Discussion

CML provides an appropriate disease model for multistep carcinogenesis in which generation of p210BCR/ABL initiates CML CP and an additional genetic event(s) contributes to the evolution to CML BC.[8] We developed a transgenic mouse model for human CML, which expresses *p210BCR/ABL* in hematopoietic progenitor cells and reproducibly exhibits a CML-like myeloproliferative disorder.[14] To investigate molecular mechanism(s) responsible for disease progression, the *p210BCR/ABL* transgenic mice were subjected to retroviral insertional mutagenesis. BXH2 mice that harbor a horizontally transmittable replication-competent retrovirus[22] were used as a virus donor strain, because it has been successfully used to detect second hit genes in previous studies.[37-39]

The inbred BXH2 mice were reported to develop acute myeloid leukemia at 7 to 12 months of age due to ecotropic virus integration and intrinsic myeloid tropism.[22-24] In line with this report, all the WT/BXH2 mice died of myeloid leukemia (Figure 1A). In contrast, 6 p210BCR/ABL/BXH2 mice developed nonmyeloid leukemias with a shorter latency. The early disease onset and different phenotypes in these mice indicated that the diseases were caused by the cooperation of *p210BCR/ABL* with altered expression of virus-affected gene(s). Therefore, in this study, we intended to identify virus-integrated genes in the tumors of the 6 mice and iPCR analysis detected 2 CISs in B-cell leukemia samples. These CISs were considered to be strong candidates for CML BC, because leukemia with B-cell phenotype has not been detected in *p210BCR/ABL* transgenic mice[14] and very rarely reported in BXH2 mice (http://rtcgd.abcc.ncifcrf.gov/).[22,23,27]

It is to be noted that one CIS was in the promoter region of the transgene. Interestingly, our previous retrovirus insertional mutagenesis study, in which newborn *p210BCR/ABL* transgenic mice were directly injected with retroviruses, also identified the transgene as a CIS in B-cell BC cases, where retrovirus integration resulted in overexpression and/or enhanced kinase activity of the transgene product.[40] The up-regulation of *p210BCR/ABL* in the blast phase is especially interesting, because it corresponds to double Ph, which is one of the most frequently observed chromosomal abnormalities found in CML BC.[8] Therefore, our observation provides in vivo experimental evidence that acquired enhancement of *p210BCR/ABL* expression accelerates the disease and causes BC. The reason why mice with transgene integration exhibited B-cell leukemia is not clear. It could be possible that *p210BCR/ABL* originally expressed by the *TEC* promoter and then up-regulated by retrovirus insertion might predispose the infected mice to develop B-ALL by an unknown mechanism. In human CML BC, double Ph was reported to be occasionally associated with B-cell BC samples.[41,42]

Another CIS was the 5′ noncoding region of *Zfp423,* which encodes a transcription factor with multiple zinc-finger repeats.[33] Zfp423 was originally identified as a binding partner of Ebf (early B-cell factor, also denoted as Olf1), a protein essential for B-cell and olfactory nervous system development,[43,44] and was subsequently shown to interact with SMADs in response to bone morphogenic protein 2 (BMP2) in the *Xenopus laevis*.[45] *Zfp423* was also cloned as a target in B-cell lymphoma in AKXD27 mice by retroviral insertional mutagenesis.[33] In that study, retrovirus integration occurred upstream of the translation initiation codon resulting in a high level of expression, as observed in our cases (Figure 2).[33] A recent study demonstrated that *Zfp423* knockout mice exhibited abnormal cerebellum development but appeared to have a normal hematopoiesis,[46] suggesting that its ectopic expression would be involved in leukemogenesis.

It remains to be clarified how overexpression of *Zfp423* contributes to B-cell malignancy. Interestingly, although Zfp423 was originally identified as an Ebf-binding partner, it is not expressed in hematopoietic tissues including B cells.[33,34] In the olfactory nervous system, Zfp423 was shown to negatively regulate Ebf function; Zfp423 forms a heterodimer with Ebf, which inhibits Ebf homodimer formation that has an ability to transactivate downstream target genes.[43] Thus, it would be possible that the aberrant expression of *Zfp423* in the hematopoietic system induces B-cell leukemia, at least in part by impairing Ebf-mediated signaling. Alternatively, because a recent study demonstrated that a highly conserved 12–amino acid peptide located in the extreme

N-terminus of Zfp423 recruits the nucleosome remodeling and deacetylase corepressor complex (NuRD),[47] it could be postulated that Zfp423 functions as a transcription repressor and contributes to leukemogenesis by suppressing downstream target genes.

In this study, *Zfp423* was identified as a gene whose deregulated expression cooperates with *p210BCR/ABL* and induces CML BC. The cooperative activities of *Zfp423* and *p210BCR/ABL* were demonstrated by in vitro and in vivo mouse experiments and also by human samples. Enforced expression of *Zfp423* in hematopoietic cells derived from *p210BCR/ABL* transgenic mice enhanced B-cell colony formation, and suppression of *ZNF423* expression in *ZNF423*-expressing, *p210BCR/ABL*-positive CML BC cells reduced cell growth (Figure 3). In addition, expression of *Zfp423* with *p210BCR/ABL* in hematopoietic progenitor cells accelerated *p210BCR/ABL*-mediated leukemia and induced a more aggressive phenotype mainly of B-cell lineage (Figure 4). Furthermore, *ZNF423* is expressed in a subset of *BCR/ABL*-positive hematopoietic cell lines and several CML BC samples mostly with B-cell phenotype (Figure 5). These results demonstrated that *Zfp423/ZNF423* cooperates with *p210BCR/ABL,* confers a proliferative advantage to *p210BCR/ABL*-expressing hematopoietic cells, and consequently develops CML B-cell BC. It is to be noted that *ZNF423* expression was detected in several Ph-negative B-ALL lines (Figure 5), which indicates that *ZNF423* contributes not only to CML B-cell BC or Ph-positive B-ALL but also to de novo B-ALL without *BCR/ABL.*

It is intriguing that while the recipient mice transduced with both *p210BCR/ABL* and *Zfp423* developed mainly B-ALL, 2 cases developed AML (Figure 4B). Although *Zfp423* has been exclusively associated with B-ALL in retroviral insertional mutagenesis studies,[33,34] this result strongly suggests that *Zfp423* might contain a potency to develop AML as well as B-ALL. This idea is in accordance with the finding that one myeloid BC case expressed *ZNF423* in clinical analysis (Figure 5B no. 6). Recently, *Zfp521/ZNF521* (also known as *EHZF [early hematopoietic zinc finger protein]* and *Evi3*), which is homologous to *Zfp423/ZNF423* and was also identified as a target of B-ALLs by mouse retrovirus insertional mutagenesis studies,[34,48] was reported to be frequently involved in AML samples in human leukemias.[49] Thus, a set of zinc finger–containing transcription factors that has been isolated as a target in B-ALL in mice might contribute to leukemias with different phenotypes in humans.

As for the 2 mice that developed T-ALL, although we could not identify any CIS, candidate genes, such as *Hcst (hematopoietic cell signal transducer,* also called *DAP10/KAP10*), an adaptor protein involved in T-cell signaling,[50,51] and *Il21r* (*IL21 receptor*), a cytokine receptor mediating T-cell activation[52,53] were detected (Table S1). In addition, several genes isolated by iPCR have been reported in cancer gene studies. For example, *Avpil1, Ddx6, Runx1, Mef2d, Jak1, Cbfa2t3h,* and *Sox4* have already been identified as retrovirus integration sites in the mouse retrovirus tagged cancer gene database (RTCGD; http://rtcgd.abcc.ncifcrf.gov/),[23,27] and *IL21R, DDx6, Runx1,* and *Cbfa2t3h* have been denoted as chromosomal translocation-associated genes in human cancer (http://www.sanger.ac.uk/genetics/CGP/Census/).[54] Furthermore, *MEF2D* was shown to create a fusion gene in t(1;19)(q23;p13),[55] and *Sox4* was demonstrated to be a powerful tool to identify cooperative genes when transplanted by a replication-defective retrovirus.[56] Further studies will be required to investigate whether virus insertion in these genes might affect the BC phenotype and/or lineage commitment observed in p210BCR/ABL/BXH2 mice.

In this study, we demonstrated that enhanced expression of *p210BCR/ABL* and aberrant expression of *Zfp423/ZNF423* contribute to blastic transformation of *p210BCR/ABL*-expressing hematopoietic cells. Our results provide insights into the molecular mechanism(s) for disease progression of human CML and prove this transgenic system is a valuable tool in identifying genes whose altered expression cooperates with *p210BCR/ABL* to induce CML BC.

Acknowledgments

We thank Yuki Sakai, Kayoko Hashimoto, and Yuko Tsukawaki for the mouse care and technical assistance; Tomoko Takahara and Yukari Yamazaki for BMT studies; and Hirotaka Matsui for the statistical analysis. We also thank Motomi Osato for helpful discussion and Hiroya Aso and Toshiya Inaba for providing us with Ph-positive human hematopoietic cell lines.

This work was supported by a Grant-in-Aid from the Ministry of Education, Science and Culture of Japan (Tokyo, Japan), a Grant-in-Aid for Cancer Research from the Ministry of Health, Labor and Welfare of Japan (13-2; Tokyo, Japan) Research Grant of the Princess Takamatsu Cancer Research Fund (Tokyo, Japan), Mitsubishi Pharma Research Foundation (Osaka, Japan), YASUDA Medical Research Foundation (Osaka, Japan), a Grant-in-Aid of The Japan Medical Association (Tokyo, Japan), and Japan Leukemia Research Fund (Tokyo, Japan).

Authorship

Contribution: K.M., N.Y., M.M., T.N., and H.H. designed and performed the research and wrote the paper; H.O. centralized the pathologic analysis; Y. Komeno, J.K., Z.-i.H., and T. Kitamura, performed the retrovirus and shRNA studies; S.W., N.A.J., and N.G.C. participated in the Zfp423 studies and wrote the paper; T. Kuwata, Y. Kanno, and T.N. contributed to the BMT analysis; and all the authors checked and agreed on the final version of the paper.

Conflict-of-interest disclosure: The authors declare no competing financial interests.

Correspondence: Hiroaki Honda, Department of Developmental Biology, Research Institute of Radiation Biology and Medicine, Hiroshima University, 1-2-3 Kasumi, Minami-ku, Hiroshima 734-8553, Japan; e-mail: hhonda@hiroshima-u.ac.jp.

References

1. Deininger MWN, Goldman JM, Melo JV. The molecular biology of chronic myeloid leukemia. Blood. 2000;96:3343-3356.
2. Ren R. Mechanisms of BCR-ABL in the pathogenesis of chronic myelogenous leukaemia. Nat Rev Cancer. 2005;5:172-183.
3. Rowley JD. A new consistent chromosomal abnormality in chronic myelogenous leukemia identified by quinacrine fluorescence and Giemsa staining. Nature. 1973;243:290-293.
4. de Klein A, van Kessel AG, Grosveld G, et al. A cellular oncogene is translocated to the Philadelphia chromosome in chronic myelocytic leukaemia. Nature. 1982;300:765-767.
5. Groffen J, Stephenson JR, Heisterkamp N, deKlein A, Bartram CR, Grosveld G. Philadelphia chromosomal breakpoints are clustered within a limited region, bcr, on chromosome 22. Cell. 1984;36:93-99.
6. Shtivelman E, Lifshitz B, Gale RP, Canaani E. Fused transcript of abl and bcr genes in chronic myelogenous leukaemia. Nature. 1985;315:550-554.
7. Konopka JB, Watanabe SM, Witte ON. An alternation of the human c-abl protein in K562 leukemia cells unmasks associated tyrosine kinase activity. Cell. 1984;37:1035-1042.

8. Calabretta B, Perrotti D. The biology of CML blast crisis. Blood. 2004;103:4010-4022.
9. Pear WS, Miller JP, Xu L, et al. Efficient and rapid induction of a chronic myelogenous leukemia-like myeloproliferative disease in mice receiving P210 bcr/abl-transduced bone marrow. Blood. 1998;92: 3780-3792.
10. Zhang X, Ren R. Bcr-Abl efficiently induces a myeloproliferative disease and production of excess interleukin-3 and granulocyte-macrophage colony-stimulating factor in mice: a novel model for chronic myelogenous leukemia. Blood. 1998;92:3829-3840.
11. Li S, Ilaria RLJ, Million RP, Daley GQ, Van Etten RA. The P190, P210, and P230 forms of the BCR/ABL oncogene induce a similar chronic myeloid leukemia-like syndrome in mice but have different lymphoid leukemogenic activity. J Exp Med. 1999;189:1399-1342.
12. Honda H, Fujii T, Takatoku M, et al. Expression of p210bcr/abl by metallothionein promoter induced T-cell leukemia in transgenic mice. Blood. 1995; 85:2853-2861.
13. Voncken JW, Kaartinen V, Pattengale PK, Germeraad WTV, Groffen J, Heisterkamp N. BCR/ABL p210 and p190 cause distinct leukemia in transgenic mice. Blood. 1995;86:4603-4611.
14. Honda H, Oda H, Suzuki T, et al. Development of acute lymphoblastic leukemia and myeloproliferative disorder in transgenic mice expressing p210bcr/abl: a novel transgenic model for human Ph1-positive leukemias. Blood. 1998;91:2067-2075.
15. Huettner CS, Zhang P, Van Etten RA, Tenen DG. Reversibility of acute B-cell leukaemia induced by BCR-ABL1. Nat Genet. 2000;24:57-60.
16. Huettner CS, Koschmieder S, Iwasaki H, et al. Inducible expression of BCR/ABL using human CD34 regulatory elements results in a megakaryocytic myeloproliferative syndrome. Blood. 2003;102:3363-3370.
17. Koschmieder S, Gottgens B, Zhang P, et al. Inducible chronic phase of myeloid leukemia with expansion of hematopoietic stem cells in a transgenic model of BCR-ABL leukemogenesis. Blood. 2005;105:324-334.
18. Honda H, Yamashita Y, Ozawa K, HM. Cloning and characterization of mouse tec promoter. Biochem Biophys Res Commun. 1996;223:422-426.
19. Honda H, Ozawa K, Yazaki Y, Hirai H. Identification of PU. 1 and Sp1 as essential transcriptional factors for the promoter activity of mouse tec gene. Biochem Biophys Res Comm. 1997;234: 376-381.
20. Honda H, Ushijima T, Wakazono K, et al. Acquired loss of p53 induces blastic transformation in p210bcr/abl-expressing hematopoietic cells: a transgenic study for blast crisis of human CML. Blood. 2000;95:1144-1150.
21. Niki M, Cristofano DA, Zhao M, et al. Role of Dok-1 and Dok-2 in leukemia suppression. J Exp Med. 2004;200:1689-1695.
22. Li J, Shen H, Himmel KL, et al. Leukaemia disease genes: large-scale cloning and pathway predictions. Nat Genet. 1999;23:348-353.
23. Akagi K, Suzuki T, Stephens RM, Jenkins NA, Copeland NG. RTCGD: retroviral tagged cancer gene database. Nucleic Acids Res. 2004;32(database issue):D523-D527.
24. Turcotte K, Gauthier S, Tuite A, Mullick A, Malo D, Gros P. A mutation in the Icsbp1 gene causes susceptibility to infection and a chronic myeloid leukemia-like syndrome in BXH-2 mice. J Exp Med. 2005;201:881-890.
25. Miyazaki K, Kawamoto T, Tanimoto K, Nishiyama M, Honda H, Kato Y. Identification of functional hypoxia response elements in the promoter region of the DEC1 and DEC2 genes. J Biol Chem. 2002;277:47014-47021.
26. University of Colombo School of Computing. UCSC Genome Browser. http://genome.ucsc.edu. Accessed January 2009.
27. National Cancer Institute–Frederick. Mouse Retrovirus Tagged Cancer Gene Database. http://rtcgd.abcc.ncifcrf.gov. Accessed January 2009.
28. Kitamura T, Koshino Y, Shibata F, et al. Retrovirus-mediated gene transfer and expression cloning: powerful tools in functional genomics. Exp Hematol. 2003;31:1007-1014.
29. Morita S, Kojima T, Kitamura T. Plat-E: an efficient and stable system for transient packaging of retroviruses. Gene Ther. 2000;7:1063-1066.
30. Jin G, Yamazaki Y, Takuwa M, et al. Trib1 and Evi1 cooperate with Hoxa and Meis1 in myeloid leukemogenesis. Blood. 2007;109:3998-4005.
31. Kono H, Kyogoku C, Suzuki T, et al. FcgamaRIIB Ile232Thr transmembrane polymorphism associated with human systemic lupus erythematosus decreases affinity to lipid rafts and attenuates inhibitory effects on B cell receptor signaling. Hum Mol Genet. 2005;14:2881-2892.
32. Harada H, Harada Y, Tanaka H, Kimura A, Inaba T. Implications of somatic mutations in the AML1 gene in radiation-associated and therapy-related myelodysplastic syndrome/acute myeloid leukemia. Blood. 2003;101:673-680.
33. Warming S, Suzuki T, Yamaguchi TP, Jenkins NA, Copeland NG. Early B-cell factor-associated zinc-finger gene is a frequent target of retroviral integration in murine B-cell lymphomas. Oncogene. 2004;23:2727-2731.
34. Warming S, Liu P, Suzuki T, et al. Evi3, a common retroviral integration site in murine B-cell lymphoma, encodes an EBFAZ-related Kruppel-like zinc finger protein. Blood. 2003;101:1934-1940.
35. Sanuki S, Hamanaka S, Kaneko S, et al. A new red fluorescent protein that allows efficient marking of murine hematopoietic stem cells. J Gene Med. 2008;10:965-971.
36. Pane F, Intrieri M, Quintarelli C, Izzo B, Muccioli GC, Salvatore F. BCR/ABL genes and leukemic phenotype: from molecular mechanisms to clinical correlations. Oncogene. 2002;21:8652-8667.
37. Iwasaki M, Kuwata T, Yamazaki Y, et al. Identification of cooperative genes for NUP98-HOXA9 in myeloid leukemogenesis using a mouse model. Blood. 2005;105:784-793.
38. Yanagida M, Osato M, Yamashita N, et al. Increased dosage of Runx1/AML1 acts as a positive modulator of myeloid leukemogenesis in BXH2 mice. Oncogene. 2005;24:4477-4485.
39. Yamashita N, Osato M, Huang L, et al. Haploinsufficiency of Runx1/AML1 promotes myeloid features and leukaemogenesis in BXH2 mice. Br J Haematol. 2005;131:495-507.
40. Mizuno T, Yamasaki N, Miyazaki K, et al. Overexpression/enhanced kinase activity of BCR/ABL and altered expression of Notch1 induced acute leukemia in p210BCR/ABL transgenic mice. Oncogene. 2008;27:3465-3474.
41. Tien HF, Chuang SM, Wang CH, et al. Chromosomal characteristics of Ph-positive chronic myelogenous leukemia in transformation: a study of 23 Chinese patients in Taiwan. Cancer Genet Cytogenet. 1989;39:89-97.
42. Griesshammer M, Heinze B, Bangerter M, Heimpel H, Fliedner TM. Karyotype abnormalities and their clinical significance in blast crisis of chronic myeloid leukemia. J Mol Med. 1997;75: 836-838.
43. Tsai RY, Reed RR. Cloning and functional characterization of Roaz, a zinc finger protein that interacts with O/E-1 to regulate gene expression: implications for olfactory neuronal development. J Neurosci. 1997;17:4159-4169.
44. Tsai RY, Reed RR. Identification of DNA recognition sequences and protein interaction domains of the multiple-Zn-finger protein Roaz. Mol Cell Biol. 1998;18:6447-6456.
45. Hata A, Seoane J, Lagna G, Montalvo E, Hemmati-Brivanlou A, Massague J. OAZ uses distinct DNA- and protein-binding zinc fingers in separate BMP-Smad and Olf signaling pathways. Cell. 2000;100:229-240.
46. Warming S, Rachel RA, Jenkins NA, Copeland NG. Zfp423 is required for normal cerebellar development. Mol Cell Biol. 2006;26: 6913-6922.
47. Lauberth SM, Rauchman MA. Conserved 12-amino acid motif in Sall1 recruits the nucleosome remodeling and deacetylase corepressor complex. J Biol Chem. 2006;281:23922-23931.
48. Hentges KE, Weiser KC, Schountz T, Woodward LS, Morse HC, Justice MJ. Evi3, a zinc-finger protein related to EBFAZ, regulates EBF activity in B-cell leukemia. Oncogene. 2005; 24:1220-1230.
49. Bond HM, Mesuraca M, Amodio N, et al. Early hematopoietic zinc finger protein-zinc finger protein 521: a candidate regulator of diverse immature cells. Int J Biochem Cell Biol. 2008;40:848-854.
50. Wu J, Song Y, Bakker AB, et al. An activating immunoreceptor complex formed by NKG2D and DAP10. Science. 1999;285:730-732.
51. Chang C, Dietrich J, Harpur AG, et al. Cutting edge: KAP10, a novel transmembrane adapter protein genetically linked to DAP12 but with unique signaling properties. J Immunol. 1999; 163:4651-4654.
52. Mehta DS, Wurster AL, Grusby MJ. Biology of IL-21 and the IL-21 receptor. Immunol Rev. 2004; 202:84-95.
53. Leonard WJ, Spolski R. Interleukin-21: a modulator of lymphoid proliferation, apoptosis and differentiation. Nat Rev Immunol. 2005;5:688-698.
54. Wellcome Trust Sanger. Cancer Gene Census. http://www.sanger.ac.uk/genetics/CGP/Census. Accessed _.
55. Yuki Y, Imoto I, Imaizumi M, et al. Identification of a novel fusion gene in a pre-B acute lymphoblastic leukemia with t(1;19)(q23;p13). Cancer Sci. 2004;95:503-507.
56. Du Y, Spence SE, Jenkins NA, Copeland NG. Cooperating cancer-gene identification through oncogenic-retrovirus-induced insertional mutagenesis. Blood. 2005;106:2498-2505.

Biochemical and Biophysical Research Communications 390 (2009) 65–70

Contents lists available at ScienceDirect

Biochemical and Biophysical Research Communications

journal homepage: www.elsevier.com/locate/ybbrc

Wnt modulators, SFRP-1, and SFRP-2 are expressed in osteoblasts and differentially regulate hematopoietic stem cells

Hideaki Nakajima [a,b,*], Miyuki Ito [b], Yoshihiro Morikawa [c], Tadasuke Komori [c], Yumi Fukuchi [a,b], Fumi Shibata [d], Shinichiro Okamoto [a], Toshio Kitamura [d]

[a] Division of Hematology, Department of Internal Medicine, Keio University School of Medicine, Tokyo 160-8582, Japan
[b] Center of Excellence, Institute of Medical Science, University of Tokyo, Tokyo 108-8639, Japan
[c] Department of Anatomy and Neurobiology, Wakayama Medical College, Wakayama 641-8509, Japan
[d] Division of Cellular Therapy, Advanced Clinical Research Center, Institute of Medical Science, University of Tokyo, Tokyo 108-8639, Japan

ARTICLE INFO

Article history:
Received 15 September 2009
Available online 22 September 2009

Keywords:
Hematopoietic stem cells
Secreted frizzled-related protein
SFRP
Wnt
Self-renewal
Osteoblast

ABSTRACT

Wnt signaling has been implicated in the self-renewal of hematopoietic stem cells (HSCs). Secreted frizzled-related proteins (SFRPs) are a family of soluble proteins containing a region homologous to a receptor for Wnt, Frizzled, and are thought to act as endogenous modulators for Wnt signaling. This study examined the role of SFRPs in HSC regulation. Among the four family members, SFRP-1 and SFRP-2 are specifically induced in the bone marrow in response to myelosuppression, and immunostaining revealed that both proteins were expressed in osteoblasts. Interestingly, SFRP-1 reduced the number of multipotent progenitors in *in vitro* culture of $CD34^-KSL$ cells, while SFRP-2 did not. Furthermore, SFRP-1 compromised the long-term repopulating activity of HSCs, whereas SFRP-2 did not affect or even enhanced it in the same setting. These results indicate that although both SFRP-1 and SFRP-2 act as inhibitors for Wnt signaling *in vitro*, they differentially affect the homeostasis of HSCs.

Introduction

Hematopoietic stem cells (HSC) are a rare population of cells that are capable of supporting life-long hematopoiesis [1]. They are characterized by the unique capacity to self-renew and differentiate into all blood cell lineages. The molecular mechanisms controlling self-renewal of HSCs have not yet been fully elucidated, but previous reports suggest that the Wnt family of proteins is implicated in this process [2].

Wnts are a family of secreted proteins that are involved in a variety of biological and pathological processes such as skeletal development, embryogenesis, organogenesis and tumor development [3,4]. Frizzled (Fz) family proteins serve as receptors for Wnt, and Wnt binding to Fz forms receptor complex with or without low-density lipoprotein receptor related protein (LRP)-5 or -6 to activate canonical or non-canonical signaling pathways. There are a number of endogenous Wnt regulators, such as secreted Frizzled-related protein (SFRP), WIF-1, Cerberus, and Dickkopf (Dkk)[5]. SFRPs contain a characteristic cysteine-rich domain (CRD) in the N-terminus which shares homology with CRD of Fz [5–7]. Since CRD of Fz serves as a binding surface for Wnt, SFRPs are speculated to modulate the Wnt-Fz interactions through its CRD; however, the physiological impact of SFRPs on Wnt signaling still remains to be elucidated. Previous studies have indicated that mammalian SFRPs were repressors of the canonical Wnt pathway when they are overexpressed *in vitro* [8–10], while other studies have shown the agonistic function of SFRP-1 for Wnt signaling [11], thus suggesting a context-dependent action of SFRPs. During embryonic development, SFRPs and Wnts are expressed in either distinct or sometimes overlapping areas, thereby coordinating overall Wnt activities critical for appropriate organogenesis [6,12–16]. Due to their putative Wnt-inhibitory activity, SFRPs have been postulated to serve as tumor suppressors. Indeed, some SFRPs have been reported to be inactivated by either promoter hypermethylation or chromosomal deletion in certain types of cancers [8,17,18].

Although Wnts, especially Wnt3a, have been reported to play critical roles in the self-renewal of HSCs, little is known about the roles of Wnt modulators in the HSC physiology. This study investigated the effects of SFRP-1 and SFRP-2 on the differentiation, proliferation, and self-renewal of HSCs. The results suggest SFRP-1 and SFRP-2 are differentially involved in the homeostasis of HSCs.

Materials and methods

Mice. C57BL/6 (B6) mice were from Japan CLEA Inc. (Tokyo, Japan), and B6-Ly5.1 mice were from Sankyo Lab Service Co.

* Corresponding author. Address: Division of Hematology, Department of Internal Medicine, Keio University School of Medicine, 35 Shinanomachi, Shinjuku-ku, Tokyo 160-8582, Japan. Fax: +81 3 3353 3515.
E-mail address: hnakajim@sc.itc.keio.ac.jp (H. Nakajima).

0006-291X/$ - see front matter © 2009 Elsevier Inc. All rights reserved.
doi:10.1016/j.bbrc.2009.09.067

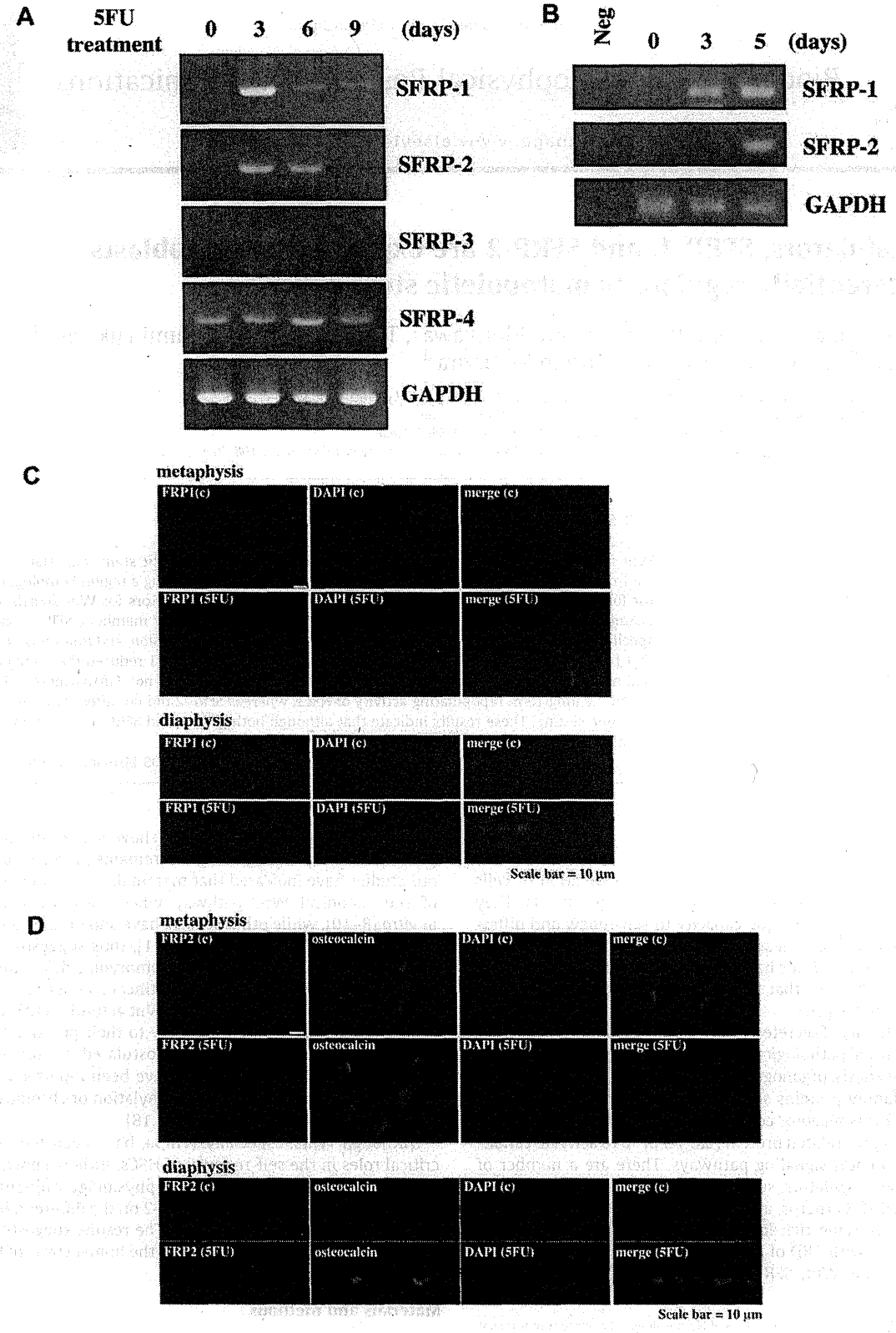

Fig. 1. Expression of SFRP-1 and SFRP-2 in osteoblasts. (A,B) Expression of the SFRP family genes in the BM and their regulation by myelosuppression. The mice were treated with 5-FU (150 mg/kg, i.p.) (A) or irradiation (950 rads) (B), and the BM cells were harvested at the indicated time points. The expressions of SFRP genes in the whole BM cells were analyzed by RT-PCR. PCR was run for 35 cycles. (C,D) The sections of femurs prepared from either control non-treated mice (C) or mice treated with 5-FU for 3 days (5-FU) were immunostained with anti-SFRP-1 (FRP1) (C) or SFRP-2 (FRP2) (D) antibodies. SFRP-2 was stained together with an anti-osteocalcin antibody. In (C), double staining of SFRP-1 and osteocalcin was not possible since both antibodies were from the same species. The nuclei were counterstained with DAPI.

(Tsukuba, Japan). Mice from 8 to 12 weeks old were used in all experiments. All animal experiments were reviewed and approved by the Internal Review Board of the Institute of Medical Science, the University of Tokyo and by the Committee of Animal Use and Care of Keio University School of Medicine.

Reagents. Recombinant human SFRP-1, mouse SFRP-2, and mouse Wnt3a proteins were purchased from R&D systems.

Flow cytometry. The following monoclonal antibodies were used for flow cytometric analysis: c-Kit (ACK2), Sca-1 (E13-161.7), and CD34 (RAM34). All antibodies were purchased from BD Pharmingen. Purification of $CD34^-KSL$ cells was done as previously described [19]. Briefly, BM cells were harvested from 8- to 12-week-old mice, and mononuclear cells were separated by density-gradient centrifugation using Lymphoprep (Nycomed). Lineage-positive cells were depleted with Lineage Cell Depletion Kit (Miltenyi Biotec) according to the manufacturer's protocol. Lineage-negative cells were stained with anti-CD34-FITC, anti-Sca-1-PE, anti-c-Kit-APC, and an anti-lineage antibody cocktail in the Lineage Cell Depletion Kit, followed by staining with streptoavidin-PE-Cy7. FACS Calibur or FACS Aria was used for analysis and cell sorting.

Culture of hematopoietic stem cells and colony-forming assays. $CD34^-KSL$ cells were sorted into 96-well plates and cultured in S-clone SF-03 (Sanko Junyaku) + 0.5% bovine serum albumin (BSA) + 50 ng/ml SCF + 50 ng/ml TPO with or without 1 μg/ml of recombinant SFRP-1 or SFRP-2 (R&D systems). Colony-forming assays were performed as previously described [20]. Cells were recovered, cytospun onto glass slides, and then subjected to May-Giemsa staining for morphological examination.

Bone marrow transplantation. Cultured $CD34^-KSL$ cells from C57BL/6-Ly5.1 mice were transplanted into lethally irradiated (950 rad) C57BL/6-Ly5.2 recipients in competition with 2×10^5 BM mononuclear cells from Ly5.2 mice. Reconstitution of donor cells in peripheral blood was monitored by staining cells with anti-Ly5.1 antibody. Secondary transplantation was performed by injecting 2×10^6 whole BM cells taken from primary recipient mice at 24-weeks after the first transplant into lethally irradiated C57BL/6-Ly5.2 secondary recipients.

RT-PCR. $PolyA^+$ mRNA was extracted from BM cells using a Micro-FastTrack 2.0 Kit (Invitrogen). cDNAs were reverse-transcribed by SuperScript II reverse transcriptase (Invitrogen), and PCR was performed with Ex Taq-HS (Takara). Primer sequences are shown in Supplementary Table 1.

Immunostaining. Mice treated with 5-FU (150 mg/kg, i.p.) for 3 days were fixed by perfusing Zamboni's fixative. Femurs were then dissected and decalcified in 10% EDTA at 4 °C. The bones were embedded in OCT compound (Sakura Fine Technical, Tokyo, Japan), frozen, and sectioned in 5 μm thick by Cryostat (Leica). Sections were blocked with biotin and normal donkey serum, and stained with rabbit anti-FRP-1 (H-90, Santa Cruz), goat anti-FRP-2 (C-18, Santa Cruz), and anti-osteocalcin (Takara) antibodies, which were then subjected to secondary staining with anti-rabbit or goat IgG-biotin and anti-mouse IgG-Cy3, and tertiary staining with streptoavidin-Cy2. Sections were washed three times for 5 min in PBS between each step and finally mounted in Vectashield anti-fading medium (Vector Labs; Burlingame, CA) containing DAPI (Sigma Chemical; St. Louis, MO) for nuclear labeling. Fluorescent images were examined and captured by laser confocal microscope (Olympus).

Plasmids. Retroviral plasmid expressing mouse SFRP-1 (pMXs-IG/mSFRP-1) was described previously [21]. For pMXs-IG/mSFRP-2, cDNA was amplified by PCR with Pfu polymerase (Stratagene) using murine bone marrow cDNA as a template, and was subcloned into pMXs-IG vector. Integrity of the amplified sequence was confirmed by DNA sequencing.

Retrovirus production and infection. Production of retrovirus was performed as previously described [22]. Mice were treated with single dose of 5-FU (150 mg/kg, i.p.) and their BM cells were harvested four days after the treatment. BM mononuclear cells were separated and used for retrovirus infection. Infection of retrovirus was performed using RetroNectin (Takara) according to the manufacturer's protocol.

Statistical analysis. All statistical analyses were performed by unpaired Student's *t*-test using PRIZM software.

Results

Induction of SFRP-1 and SFRP-2 in the bone marrow by myelosuppression

The expression of SFRPs in response to myelosuppressive stress was examined to determine the role of SFRPs in the regulation of

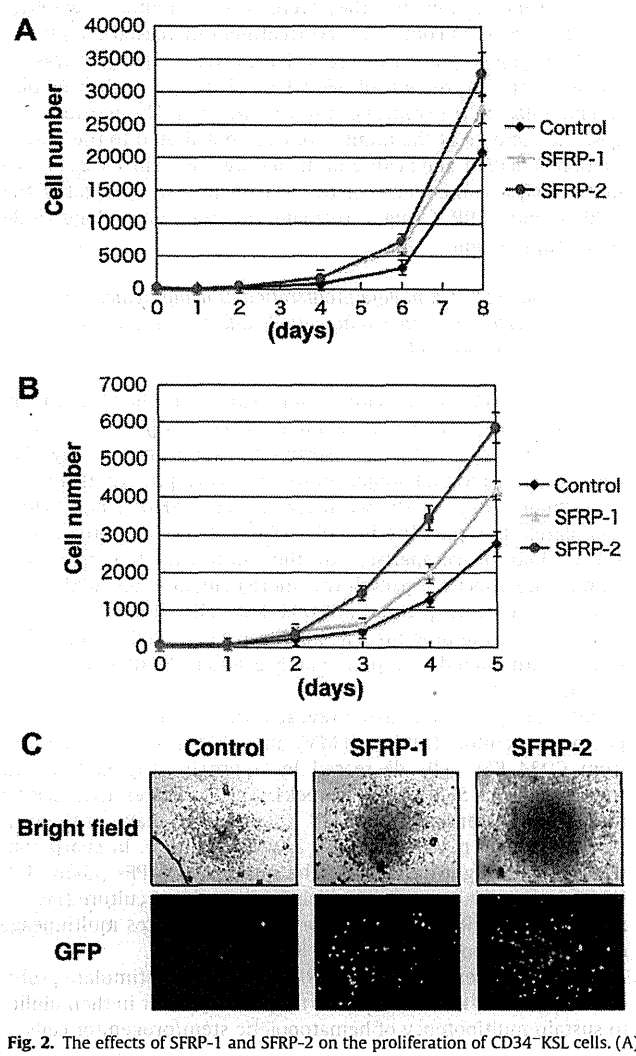

Fig. 2. The effects of SFRP-1 and SFRP-2 on the proliferation of $CD34^-KSL$ cells. (A) One hundred $CD34^-KSL$ cells/well were sorted into a 96-well plate and cultured in S-Clone SF-03 supplemented with 0.5% BSA, 50 μM 2-ME, stem cell factor (SCF, 50 ng/ml) and thrombopoietin (TPO, 50 ng/ml) with SFRP-1 (1 μg/ml) or SFRP-2 (1 μg/ml). Cell numbers were counted at each time points under a microscope ($n = 3$, mean ± S.D.). (B) One hundred $CD34^-KSL$ cells were sorted into a 96-well plate coated with RetroNectin, and prestimulated in αMEM supplemented with 1% FBS, 50 ng/ml SCF, 50 ng/ml TPO and 50 μM 2-mercaptoethanol (2-ME). Control-, SFRP-1- or SFRP-2-retrovirus was added after 24 h of prestimulation; the cells were further cultured in S-clone SF-03 containing 0.5% BSA, 50 ng/ml SCF, 50 ng/ml TPO and 50 μM 2-ME. GFP^+ cell numbers were counted at the indicated time points (upper panel). Data are means ± S.D. ($n = 3$). Representative pictures of cells cultured for five days were also shown (lower panel, original magnification, 100×).